X-Ray Scaling Relations of Galaxy Groups in a Hydrodynamic Cosmological Simulation

Romeel Davé [1]

Steward Observatory, University of Arizona, Tucson, AZ 85721

Neal Katz

Astronomy Department, University of Massachusetts, Amherst, MA 01003

and

David H. Weinberg

Astronomy Department, Ohio State University, Columbus, OH 43210

ABSTRACT

We examine the scalings of X-ray luminosity, temperature, and dark matter or galaxy velocity dispersion for galaxy groups in a ΛCDM cosmological simulation, which incorporates gravity, gas dynamics, radiative cooling, and star formation, but no substantial non-gravitational heating. In agreement with observations, the simulated $L_X - \sigma$ and $L_X - T_X$ relations are steeper than those predicted by adiabatic simulations or self-similar models, with $L_X \propto \sigma^{4.4}$ and $L_X \propto T_X^{2.6}$ for massive groups and significantly steeper relations below a break at $\sigma \approx 180$ km/s ($T_X \approx 0.7$ keV). The $T_X - \sigma$ relation is fairly close to the self-similar scaling relation, with $T_X \propto \sigma^{1.75}$, provided that the velocity dispersion is estimated from the dark matter or from $\gtrsim 10$ galaxies. The entropy of hot gas in low mass groups is higher than predicted by self-similar scaling or adiabatic simulations, and it agrees with observational data that suggest an "entropy floor." The steeper scalings of the luminosity relations are driven by radiative cooling, which reduces the hot (X-ray emitting) gas fraction from 50% of the total baryons at $\sigma \approx 500$ km/s to 20% at $\sigma \approx 100$ km/s. A secondary effect is that hot gas in smaller systems is less clumpy, further driving down L_X. A smaller volume simulation with eight times higher mass resolution predicts nearly identical X-ray luminosities at a given group mass, demonstrating the insensitivity of the predicted scaling relations to numerical resolution. The higher resolution simulation predicts *higher* hot gas fractions at a given group mass, and these predicted fractions are in excellent agreement with available observations. There remain some quantitative discrepancies: the predicted mass scale of the $L_X - T_X$ and $L_X - \sigma$ breaks is somewhat too low, and the luminosity-weighted temperatures are too high at a given σ, probably because our simulated temperature profiles are flat or rising towards small radii while observed profiles decline at $r \lesssim 0.2 R_{\rm vir}$. We conclude that radiative cooling has an important quantitative impact on group X-ray properties and can account for many of the observed trends that have been interpreted as evidence for non-gravitational heating. Improved simulations and observations are needed to understand the remaining discrepancies and to decide the relative importance of cooling and non-gravitational heating in determining X-ray scalings.

Subject headings: cosmology: observations — cosmology: theory — X-rays: galaxies: clusters — galaxies: clusters: general

1

1. Introduction

Galaxy groups, i.e. bound systems having typically a few $L_\star$ galaxies, contain the majority of galaxies in the Universe, and hence seem crucial to understanding the processes of galaxy formation. However, observational and theoretical studies have tended to focus either on the smaller scale of individual galaxies or on the larger scale of rich clusters. Groups present an observational challenge, since projection effects make them difficult to identify unambiguously in optical imaging surveys and their X-ray emission is faint, emerging predominantly at lower energies that are contaminated by foreground Galactic emission. Sensitive X-ray instruments and group catalogs created from large redshift surveys are transforming this observational situation, and they have revealed puzzling departures in the group mass regime from the scaling relations obeyed by rich clusters. In this paper we use a large hydrodynamic cosmological simulation to examine the predicted X-ray scaling relations of galaxy groups, reaching to the mass regime of poor clusters. We adopt an inflationary cold dark matter scenario with a cosmological constant (ΛCDM).

The canonical approach to understanding groups treats them as scaled down versions of rich clusters. The simplest model of a cluster, in turn, is a sphere of Virial-temperature gas punctuated by old galaxies, with perhaps a cooling flow onto the central cD galaxy. In this model, the gas cooling time is longer than a Hubble time everywhere except near the center, and thus it is predicted that intracluster and intragroup media should follow "self-similar" scaling relations: $T_X \propto \sigma_{\rm gal}^2$, $L_X \propto T_X^2$, and $L_X \propto \sigma_{\rm gal}^4$, where L_X is the total X-ray luminosity, T_X is the gas temperature (presumed to be the halo Virial temperature), and $\sigma_{\rm gal}$ is the velocity dispersion of cluster galaxies (presumed to trace the system's total mass). The first relation arises from equating the gas thermal energy to the galaxies' kinetic energy (i.e. hydrostatic equilibrium), the second from combining $L_X \propto MT_X^{1/2}$ for free-free emission (where M is the system mass), $M \propto \sigma_{\rm gal}^3$ from the Virial theorem, and the $T_X - \sigma_{\rm gal}$ relation, and the third from combining the previous two scaling relations

[1]Hubble Fellow, rad@as.arizona.edu

(see e.g. Navarro, Frenk, & White 1995).

While observed properties of the most massive clusters follow these relations (Allen & Fabian 1998; Xu, Jin & Wu 2001), the self-similar model breaks down as one progresses to smaller systems, with observations indicating lower than expected luminosities for a given temperature or velocity dispersion. For 207 clusters observed with *Einstein*, White, Jones, & Forman (1997) found $L_X \propto T_X^3$. Extending such observations to groups has yielded conflicting results; Mulchaey & Zabludoff (1998, hereafter MZ98) found $L_X \propto T_X^{2.8}$, consistent with clusters, while Helsdon & Ponman (2000, hereafter HP00) and Xue & Wu (2000) found much steeper relations, $L_X \propto T_X^{4.9-5.6}$.

In an influential paper, Ponman, Cannon, & Navarro (1999, hereafter PCN99) calculated the specific entropy of gas at 10% of the Virial radius, and found an "entropy floor" of $\sim 100h^{-1/3}$ keV cm^{-2} among their smallest systems. This entropy floor reduces the X-ray luminosity by lowering the gas density progressively more in smaller systems, and hence reproduces the steep $L_X - T_X$ relations seen in groups. They suggested that the entropy floor arises from energy injection by supernova winds, which might concurrently explain the enrichment level of the intracluster medium (ICM). Though there are large uncertainties for the handful of groups that demarcate the entropy floor, this result nevertheless spawned numerous papers investigating the possible physical sources of "pre-heating," constraints on parameters of the pre-heating model such as energy per baryon and energy injection redshift, and implications of pre-heating for other group and cluster observables. For instance, Lloyd-Davies, Ponman, & Cannon (2000) concluded that a temperature increase of 0.3 keV per baryon is necessary to explain the observed entropy floor, while Tozzi & Norman (2001) considered a similar uniform energy injection model and determined that the heat injection could be $\approx 0.1 - 1$ keV, depending on when and how it was injected.

Uniform heat injection across all baryons is ruled out by temperature measurements of the Lyα forest; these indicate $T \approx 2 \times 10^{-3}$ keV for most of the baryons at $z \sim 3$ (Schaye et al. 1999; Bryan 2000), and a significant fraction of baryons at $z \sim 0$ are even cooler (Ricotti, Gnedin,

& Shull 2000; Davé & Tripp 2001). Thus, heat injection must be confined in and around halos. Semi-analytic models of this scenario require much greater energy injection, typically $1-3$ keV per baryon within halos (Wu, Fabian, & Nulsen 2000; Bower et al. 2001) or entropy injection of $\sim 300 - 400$ keV cm^{-2} (Babul et al. 2002), to reproduce the PCN99 entropy floor, a result supported by adiabatic simulations of clusters with pre-heating (Bialek, Evrard, & Mohr 2001; Borgani et al. 2001). Supernovae seem unable to provide this much energy, so another energy source such as AGN-driven galactic winds is necessary (Valageas & Silk 1999; Kravtsov & Yepes 2000; Wu, Fabian, & Nulsen 2000; Bower et al. 2001; Pipino et al. 2002). While there is preliminary evidence for strong winds from Lyman break galaxies (Pettini et al. 2001), believed to evolve into cluster galaxies (Governato et al. 2001), the energy they inject seems unlikely to be as high as ~ 1 keV per baryon. The pre-heating model has also been invoked to explain the faintness of the soft X-ray background (Pen 1999; Wu, Fabian, & Nulsen 2001), though numerical simulations indicate that these constraints can probably be satisfied without non-gravitational heating (Davé et al. 2001; Phillips, Ostriker, & Cen 2001; Croft et al. 2001). In short, the pre-heating model is able to reproduce group and cluster scaling relations, but only at the expense of invoking a mysterious energy source that does not naturally arise from any firmly established physical process of galaxy formation (though see Babul et al. 2002, for some interesting hypotheses). This is the essence of the "ICM energy crisis" described by Tozzi (2001).

A fundamental assumption underlying the pre-heating model is that groups, in the absence of such heating, would be self-similarly scaled-down versions of large clusters. If some process inherent in galaxy formation breaks self-similarity, it may be that pre-heating is not required. Growing evidence suggests that radiative cooling could be this process. Bryan (2000) used an analytic model together with the observed dependence of stellar mass fraction on cluster temperature to argue that the observed scaling relations can be explained without non-gravitational heating. Voit & Bryan (2001) further argued that cooling removes low-entropy gas during the formation of cluster galaxies, leaving an effective entropy floor of ~ 100 keV cm^{-2} for groups (Voit et al. 2002). Hydrodynamic simulations support these analytic arguments. Muanwong et al. (2001) found that simulations without cooling followed the self-similar relations but that the addition of cooling steepened and lowered the $L_X - T_X$ relation, bringing it into much better agreement with observations. Thomas et al. (2002) showed that adiabatic simulations underpredict the amplitude of the $T_X - \sigma$ relation observed recently with *Chandra* but that the addition of *either* radiative cooling *or* pre-heating could resolve the discrepancy. Lewis et al. (2000) simulated a Virgo-sized cluster with and without cooling and found that the inclusion of cooling and subsequent star formation had an important impact on the X-ray emitting gas throughout the entire cluster, not just in the central region where the present-day cooling time is short. These results clearly point towards cooling as a non-negligible process in group and cluster formation, and they motivate a more thorough investigation of cooling as an alternative to pre-heating for explaining the observed scaling relations.

In this paper we analyze a cosmological hydrodynamic simulation that incorporates cooling, star formation, and (weak) feedback. Our simulation has enough dynamic range to probe the mass range from poor groups to small clusters ($\sigma \approx 100 - 550$ km/s), while resolving sub-$L_\star$ galaxies within a random cosmological volume. We describe the simulation and analysis procedures in §2. We present our simulated scaling relations in §3 and discuss the physical origin of the departures from self-similarity. We examine the average profiles of various physical quantities in our groups in §4. We go on to consider the possible effects of metallicity, velocity bias, and surface brightness thresholds in §5. These effects introduce some uncertainty in our predictions of observable scaling relations; we discuss our "best guess" predictions and compare them to observations in §5.4. Section 6 presents our conclusions. In summary, we find that radiative cooling — in particular, the greater efficiency of cooling in smaller systems — can produce departures from self-similar scaling that quantitatively mimic those of a pre-heating model. Thus, observed scaling relations do not necessarily imply that groups have experienced substantial non-gravitational heating

or entropy injection.

2. Simulation and Group Identification

We simulate a $50h^{-1}$Mpc random volume with a $7h^{-1}$kpc (equivalent Plummer, comoving) gravitational softening length, assuming a ΛCDM cosmological model with $\Omega_m = 0.4$, $\Omega_\Lambda = 0.6$, $h \equiv H_0/100 \ \mathrm{km\,s^{-1}} \ \mathrm{Mpc}^{-1} = 0.65$, $n = 0.95$, and $\sigma_8 = 0.8$. We employ 144^3 dark matter and 144^3 gas particles, yielding particle masses of $m_{\mathrm{bary}} = 8.5 \times 10^8 M_\odot$ and $m_{\mathrm{dark}} = 7.2 \times 10^9 M_\odot$. The input physics includes cooling, star formation, and thermal feedback. Because the feedback energy is deposited locally in the dense gas giving rise to star formation, it is usually radiated away quickly and produces little long-term heating of the surrounding medium. Other than this feedback, we do not inject any non-gravitational heat or entropy. The simulation was evolved from $z = 49 \rightarrow 0$ using Parallel TreeSPH (Davé et al. 1997). A detailed discussion of the algorithms, including the star formation and feedback prescriptions, is given by Katz, Weinberg, & Hernquist (1996). Relative to the simulation of Muanwong et al. (2001), who investigate similar issues with a similar numerical approach, our simulation has a mass resolution that is higher by about a factor of four and gravitational force resolution that is higher by a factor of 4–7 (depending on redshift), but a simulation volume smaller by a factor of eight. Our simulation is therefore better suited to the study of groups, but not as good for the study of rarer, more massive clusters.

We identify galaxies using SKID[2]. Our 60-particle galaxy mass resolution limit ($5 \times 10^{10} M_\odot$) corresponds to $\approx L_\star/4$, based on the equivalent number density of observed galaxies in the Sloan Digital Sky Survey (Blanton et al. 2001; for further discussion of the resolution limit and completeness threshold of the simulated galaxy sample see Murali et al. 2002). We identify bound systems using a spherical-overdensity (SO) criterion on friends-of-friends halos, as described by Gardner (2001). In this method, the most bound particle within a friends-of-friends halo is found, and the system extends radially outwards until the enclosed average density reaches the Virial density threshold (282 times the mean density for our cosmology). SO systems that contain three or more galaxies above our resolution limit are identified as "groups." We find 128 groups at $z = 0$, spanning a mass range of $10^{12.1} - 10^{14.5} M_\odot$, with up to 42 member galaxies. Note that all of these groups are bound; we identify groups in three dimensions, so our catalog does not contain chance line-of-sight projections.

To study the effects of numerical resolution, we also analyze a smaller volume, higher resolution simulation having the same cosmological model; we will refer to this as our "high-resolution" simulation. This simulation has 2×128^3 particles in a $22.222h^{-1}$Mpc volume, with $3.5h^{-1}$kpc (equivalent Plummer, comoving) softening, yielding particle masses of $m_{\mathrm{bary}} = 1.05 \times 10^8 M_\odot$ and $m_{\mathrm{dark}} = 8.8 \times 10^8 M_\odot$. We find 52 groups in this simulation at $z = 0$. By chance, this volume contains one anomalously large ($10^{14.3} M_\odot$) group containing 217 galaxies above our 60-particle galaxy mass limit of $6.3 \times 10^9 M_\odot$, but the other 51 groups probe the expected mass range down to $10^{11.2} M_\odot$.

The velocity dispersion of a group can be calculated from its dark matter (σ_{DM}) or its member galaxies (σ_{gal}). We quote 1-D velocity dispersions, obtained by dividing the 3-D velocity dispersion by $\sqrt{3}$. We find that σ_{DM} correlates tightly with group mass while σ_{gal} shows systematic deviations from σ_{DM} for smaller groups, as discussed below in §5.3.

To calculate X-ray emission, we use the latest plasma code of Raymond & Smith (1977). The interface to simulations via the TIPSY[3] package was kindly provided by G. Lewis and C. Murali. We calculate particle luminosities in the $0.5 - 2$ keV bandpass that is most commonly employed to study group X-ray properties using *ROSAT*. Unless otherwise noted, the X-ray temperature is calculated from the average luminosity-weighted temperature of group particles; we will discuss some issues relating to this in §4.3.

Applying the usual SPH formalism to obtain gas densities for calculating luminosities results in a gross overestimation of the X-ray emission. The usual SPH algorithm does a poor job of resolving the two-phase interface between the intragroup medium and gas in galaxies. As a conse-

---

[2]Spline Kernel Interpolative DENMAX, publicly available at http://www-hpcc.astro.washington.edu/tools/skid.html.

[3]Publicly available at http://www-hpcc.astro.washington.edu/tools/tipsy/tipsy

quence, the density of a hot intragroup gas particle is greatly overestimated when it happens to lie very close to a cold, dense clump, producing large and unphysical X-ray emissivities for some of the particles. To correct for this effect, we follow Pearce et al. (2000) and explicitly decouple the hot and cold phases by recalculating gas densities using only hot particles with $T > 10^5$K. Unlike Pearce et al., however, we only implement decoupling at the post-processing stage, not during the simulation itself. Our results are insensitive to the choice of temperature threshold, so long as it is below $T \lesssim 10^6$K, since virtually all gas particles bound in groups that have not cooled into galaxies have temperatures higher than this threshold. Croft et al. (2001) performed extensive tests of this approach, and found that it is indeed insensitive to the exact temperature threshold, behaves as expected with resolution, and reproduces the correct X-ray luminosity in analytic cases. The number of particles affected is small, but the total correction factors are large (typically a few to ten; see Croft et al. 2001), so our luminosity predictions must be read with this caution in mind. Additionally, since we do not explicitly decouple the hot and cold phases while evolving the simulation, we probably overpredict the amount of cooled baryons, by an uncertain amount. (The cold phase is ultimately "decoupled" from the hot phase by conversion into collisionless stars, but this conversion is not instantaneous.) Springel & Hernquist (2001) suggest that an alternative formulation of the SPH equations can resolve this "decoupling problem" in a self-consistent manner, and we will investigate this possibility in future simulations.

3. Testing Self-Similarity

3.1. Simulated Group Scaling Relations

We begin by examining whether our simulated groups follow the self-similar scaling relations expected for systems with negligible non-gravitational heating. To do this, we compute X-ray luminosities using an intragroup metallicity of zero, we sum the luminosity of all gas in the group out to its Virial radius, and we take the group's velocity dispersion to be that of the dark matter. If group formation were well described by non-radiative physics (a.k.a. "adia-

batic" physics, though gravitational shock heating is also included), then this approach should closely reproduce the self-similar scaling relations (see, e.g., Owen et al. 1998; Muanwong et al. 2001).

Figure 1, upper left, shows the $L_X - \sigma_{\mathrm{DM}}$ relation for our groups. The plot symbols indicate the number of galaxies in each group. A break is clearly evident, occurring at $\sigma_{\mathrm{DM}} \approx 180$ km/s; the fit above the break is extended to lower σ_{DM} as the dashed line, and it is clearly discrepant with these smaller systems. The dotted line shows the self-similar scaling relation, $L_x \propto \sigma_{\mathrm{DM}}^4$, normalized to our largest groups. The break value is determined by requiring continuity between the fits above and below the break. Best fit power law relations above and below this break value are listed in the lower right. Even above the break, the $L_x - \sigma_{\mathrm{DM}}$ relation is steeper than predicted by the self-similar model, with $L_X \propto \sigma_{\mathrm{DM}}^{4.7\pm0.3}$. Below the break the relation is very steep, $L_X \propto \sigma_{\mathrm{DM}}^{9.7\pm0.6}$. The fits are unweighted, to follow the procedure most commonly used by observers. We list our scaling relation fits in Table 1, including the scaling relations observed by MZ98 and HP00. We defer a comparison with observations until §5.4, where we include various observational effects in our analysis; here we simply note that the observations show a similar qualitative trend in which luminosities drop faster with decreasing group mass than the self-similar model predicts.

Figure 1, upper right, shows the $L_X - T_X$ relation. Here again a break is evident, though less obviously so, at $T \approx 0.7$ keV. Above the break, the relation is $L_X \propto T_X^{2.9\pm0.1}$, clearly discrepant with self-similarity ($L_X \propto T_x^2$, dotted line), while below the break it steepens to $L_X \propto T_X^{4.1\pm0.5}$. A single power-law fit yields a slope of 3.4 ± 0.1. Here the break value is somewhat more ambiguous, but even with the break placed at $T = 2$ keV (in which case the fits are clearly discontinuous), the slope above the break is still 2.6, and inconsistent with self-similarity. Though a double power law is an adequate fit, there is an overall trend for a continuous steepening of the relation to lower temperatures.

Our luminosity scaling relations demonstrate two points. The first is that a break occurs at all, when the simulation incorporates no physics "tuned" to pick out this mass or temperature
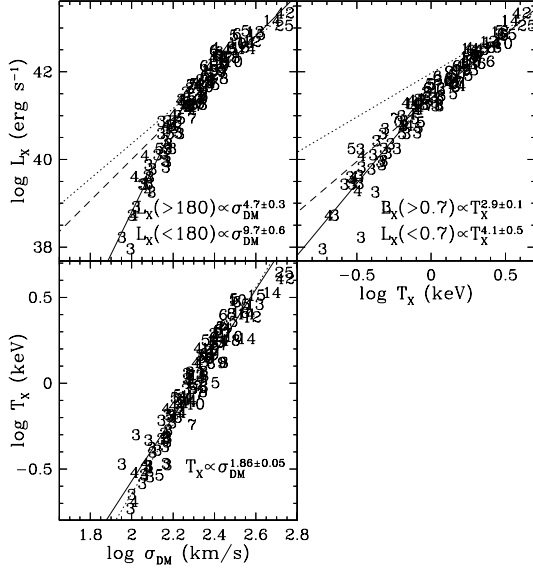
Fig. 1.— Scaling relations of the simulated galaxy groups, assuming zero metallicity. The upper left panel shows $L_X - \sigma_{\rm DM}$, upper right $L_X - T_X$, and lower left $T_X - \sigma_{\rm DM}$. The symbols indicate the number of galaxies in each group. The best-fit relations are listed in the lower right. The solid line shows the best fit, having a break at the value indicated in the legend (except in the lower left panel, where a single power law fit is acceptable). The dashed line is a continuation of the slope above the break to lower values of $\sigma_{\rm DM}$ or T_X. The dotted lines show predictions from self-similar scaling, normalized to our largest groups. These scaling relations may be compared to, e.g., Figures 4-6 of Mulchaey (2000); we will present a more detailed comparison to observations in §5.4. In no regime do our simulated luminosity scaling relations follow those predicted by self-similar models and by adiabatic numerical simulations.

scale. The second is that even above the break, the slope shows a significant departure from self-similarity. In no regime do our groups follow the expected self-similar relations, suggesting that self-similarity is an inappropriate model for relating clusters and groups. This strong departure from self-similarity is our most important result; the rest of the paper will be devoted to understanding its origin and comparing our predictions to observed group properties.

The lower left panel of Figure 1 shows the $T_X - \sigma_{\rm DM}$ relation. In contrast to the luminosity relations, this relation shows no break, and the scaling, $T \propto \sigma_{\rm DM}^{1.86 \pm 0.05}$, is only slightly off from the self-similar prediction ($T_X \propto \sigma_{\rm DM}^2$, dotted line). This agreement suggests that the X-ray temperature and dark matter velocity dispersion are both determined mainly by the gravitational potential, as expected for systems that are Virialized and in hydrostatic equilibrium. The slight excess heating that makes the relation shallower than $T_X \propto \sigma_{\rm DM}^2$ may be coming from shock heating of gas on filaments before accretion into the group potential, which can heat gas to $\sim 10^6$ K (Davé et al. 2001). Supernova feedback as implemented in this simulation is not expected to add any significant heat to the intergalactic gas. In any case, the amount of heating indicated in this plot is far from sufficient to explain the departures from self-similarity in the $L_X - T_X$ relation. Moreover, since there is no evidence of a break in $T_X - \sigma_{\rm DM}$, it is clear that some other physical process is at work in the luminosity scaling relations.

3.2. Physical Origin of the Simulated Scaling Relations

Why does our simulation yield lower-than-expected luminosities as one goes to smaller systems? The origin of this effect does not appear to be some heat source that adds pressure support and lowers the central density at a given Virial mass, nor does it appear that the low mass systems have lower luminosities because of substantially sub-Virial temperatures. Either of these scenarios would require a feature in the $T_x - \sigma$ relation close to the break at $\sigma \approx 180$ km/s in the $L_X - \sigma$ relation, and none is seen. Alternative explanations are that the X-ray emitting gas density is lowered by removal of gas from this phase, or that the density structure of the gas is changing

Table 1

Table 1

SIMULATED GROUP SCALING RELATIONS.

Z^a	SB^b	σ	$\left[\frac{d\log L_X}{d\log\sigma}\right]_{>180}$	$\left[\frac{d\log L_X}{d\log\sigma}\right]_{<180}$	$\left[\frac{d\log L_X}{d\log T_X}\right]_{>0.7}$	$\left[\frac{d\log L_X}{d\log T_X}\right]_{<0.7}$	$\left[\frac{d\log T_X}{d\log\sigma}\right]$
0	none	$\sigma_{\rm DM}$	4.7 ± 0.3	9.7 ± 0.6	2.9 ± 0.1	4.1 ± 0.5	1.86 ± 0.05
eq. 6	none	$\sigma_{\rm DM}$	4.3 ± 0.2	9.5 ± 0.6	2.5 ± 0.2	4.6 ± 0.3	1.69 ± 0.05
$0.3Z_\odot$	none	$\sigma_{\rm DM}$	3.8 ± 0.2	7.7 ± 0.5	2.2 ± 0.2	4.0 ± 0.3	1.77 ± 0.05
0	eq. 1	$\sigma_{\rm DM}$	5.0 ± 0.3	11.9 ± 0.9	3.4 ± 0.2	4.8 ± 0.4	1.88 ± 0.06
0	none	$\sigma_{\rm gal}$	3.9 ± 0.4	3.9 ± 0.9	2.9 ± 0.1	4.1 ± 0.5	1.14 ± 0.07
eq. 6	eq. 1	$\sigma_{\rm DM}$	4.4 ± 0.2	11.7 ± 0.9	2.6 ± 0.1	4.8 ± 0.4	1.75 ± 0.05
MZ98	-	-	4.3 ± 0.4	-	2.8 ± 0.1	-	2.2 ± 0.9
HP00	-	-	4.5 ± 1.1	-	4.9 ± 0.8	-	0.9 ± 0.2

[a]Assumed metallicity.

[b]Surface brightness correction.

systematically with group mass. Both of these effects are, in fact, occurring in our simulation, and together they account for the departure from the self-similar scaling relations.

The top panel of Figure 2 shows the fraction $f_{\rm hot} \equiv M_{\rm hot}/M_{\rm baryon}$ of each group's total baryons that are in the hot, X-ray emitting phase. There is a clear trend that smaller systems have less X-ray emitting gas. Our largest systems have slightly more than half of their baryons in a hot phase, while our smallest systems have less than 20%. The trend steepens slightly to smaller systems. The steepening is visually exacerbated when one plots $f_{\rm hot}^2$ on a logarithmic plot, hence the appearance of a "break" in the $L_X - T_X$ and $L_X - \sigma_{\rm DM}$ relations.

The data points in Figure 2 are binned from a compilation of observations of 30 X-ray groups and clusters with temperatures ranging from 0.8-4.5 keV. The lowest 17 are from Mulchaey et al. (1996), the next five are from Hwang et al. (1999), and the highest eight are $T < 4.5$ keV Abell clusters from Cirimele, Nesci, & Trevese (1997). The error bars shown indicate the error in the mean computed from the scatter among the data points in each bin. In each case, we take the ratio of the gaseous to gaseous+stellar mass estimates. The observations do show a trend of decreasing hot gas fraction with decreasing group mass. Unfortunately, current data do not extend to the mass range of the lowest mass groups in our simulation, where the reduction in hot gas is largest.

In the top panel of Figure 2, there appears to be remarkably good agreement between the simulated and observed hot gas fractions. Unfortunately, this agreement is somewhat misleading. As Balogh et al. (2001) have argued, X-ray observations of groups do not extend nearly as far out, relative to the virial radius, as they do in clusters, and since the hot gas is distributed more diffusely than the cold gas, the observed hot gas fraction in smaller groups is biased low. While it is difficult to correct the observations, it is possible to model this bias in our simulated groups to enable a fairer comparison. To do so, we recalculate the baryon fractions only within a radius given by

$$\frac{R_X}{R_{\rm vir}} = 1.09 \log\left(\frac{\sigma_{\rm DM}}{\rm km/s}\right) - 2.11, \qquad (1)$$

where R_X is the extent of the X-ray emission. This relation is obtained by fitting the data in Figure 3 of Mulchaey (2000) [for which we obtain $R_X/R_{\rm vir} = (\log T + 0.7)/1.7$] and using the $T_X - \sigma_{\rm DM}$ relation from Figure 1. We take $R_{\rm vir}$ to be the maximum extent of the group.

The result of applying equation (1) is shown in the second panel of Figure 2. The predicted hot fraction is indeed smaller than in the top panel, increasingly so for smaller systems. Thus, in a fairer comparison with data, our simulation appears to
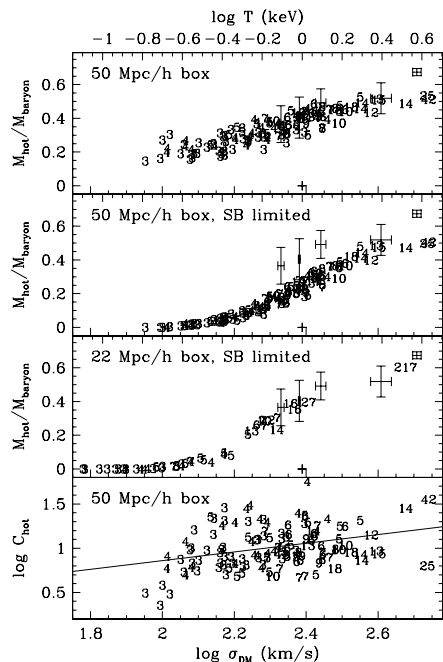
Fig. 2.— *Top panel:* Ratio of hot $(T > 10^5 \text{K})$ to total baryons as a function of group velocity dispersion. The top axis legend indicates the approximate group temperature, obtained by using the $T_X - \sigma_{\text{DM}}$ scaling relation found in Figure 1. The data points show binned observational values as described in the text. *Second panel:* Same as top panel, but results have been computed only out to an "observable" fraction of the Virial radius, as given by equation (1). *Third panel:* Same as second panel, but based on the high-resolution, smaller volume simulation. *Fourth panel:* "Clumping factor" (eq. 2) of hot gas in each group, from the large-volume simulation.

"overcool" baryons in groups. As we have discussed elsewhere (Davé et al. 2001; Murali et al. 2002), the simulation also appears to "overcool" baryons globally — the fraction of baryons converted to stars is 24%, which is high compared to estimates from the observed luminosity function (Blanton et al. 2001; Cole et al. 2001), though it is consistent with estimates from the extragalactic background light (Bernstein, Freedman, & Madore 2001).

Pearce et al. (2000) and Balogh et al. (2001) have argued that a higher resolution simulation should produce substantially more cooled gas. We can test this expectation directly using our high-resolution simulation. The third panel of Figure 2 shows the hot fraction for the 52 groups identified in this simulation, including the surface brightness cut described above. Interestingly, the trend is opposite to that argued previously: there is actually somewhat *more* hot gas in the higher resolution simulation. We believe that this increase in hot gas fraction with increasing numerical resolution, i.e. a decrease in galaxy masses, is caused by the difficulty in resolving the interface of two such distinct phases. This causes cooling rates in the immediate vicinity of galaxies to be overestimated (see §2), and affects a smaller fraction of particles in the higher resolution simulation. The hot gas fractions in our high-resolution simulation, including surface brightness bias, are in good agreement with the observations, though the range of overlap is still limited, and we do not have a still higher resolution simulation with which to demonstrate convergence of the numerical prediction. The *global* cold fraction in the high-resolution simulation is slightly higher than that of the large-volume simulation, with 26% of the baryons converted to stars, since the simulation resolves cooling and star formation further down the mass function. An estimate of the total stellar mass fraction, obtained by combining together several simulations of varying volume and resolution is presented in Fardal et al. (2002 in preparation).

The simple uniform removal of hot gas is not sufficient to fully explain the reduced luminosities of lower mass groups. Consider groups with $T_X \approx 3$ keV ($\log T \approx 0.5$), having hot gas fractions ~ 0.5, and those with $T_X \approx 0.3$ keV, having hot gas fractions ~ 0.2. Relative to a model with

constant gas fraction, the low mass groups in our simulation have hot gas densities lower by a factor of 2.5. Since $L_X \propto n_{\mathrm{hot}}^2$, this reduction should depress the luminosities of the low mass groups by a factor of 6.25. However, the gap between our best-fit relation and the self-similar scaling (solid and dotted lines of Figure 1, at $\log T_X = -0.5$) is approximately a factor of 25. This shows that the *uniform* removal of gas accounts for somewhat more than half (logarithmically) of the reduction in luminosity.

The remaining factor arises because hot gas is less clumped in the smaller systems. The bottom panel of Figure 2 shows the clumping factor

$$C_{\mathrm{hot}} = \frac{\langle \rho_{\mathrm{hot}}^2 \rangle}{\langle \rho_{\mathrm{hot}} \rangle^2} = \frac{\sum_{i=1}^{N_{\mathrm{hot}}} \rho_i}{N_{\mathrm{hot}} \bar{\rho}_{\mathrm{hot}}}, \qquad (2)$$

for each of our systems. The $\langle .. \rangle$ in the first equality represent volume averages, and the second equality expresses this ratio as a sum over (equal mass) SPH particles, where ρ_i is the SPH-estimated density of particle i, N_{hot} is the number of hot gas particles in the group, and $\bar{\rho}_{\mathrm{hot}}$ is the mean density of hot gas, namely the total hot gas mass of the group divided by the volume out to the Virial radius. If the hot gas in these groups were isothermal, then this clumping factor would be directly proportional to the luminosity (cf. Evrard et al. 1996), since the volume emissivity is proportional to ρ_{hot}^2 throughout the group. If C_{hot} were the same in high and low mass groups, then their relative luminosities would scale in proportion to f_{hot}^2 (plus temperature factors, but the group temperatures *do* follow the self-similar scaling to a good approximation). The term "clumping factor" should be applied with some caution, since the globally averaged quantity defined in equation (2) could be different in two groups that have smooth gas distributions but different radial density profiles $\rho_{\mathrm{hot}}(r)$.

Figure 2 shows that C_{hot} drops by a factor of ~ 3 from 3 keV systems to 0.3 keV systems (according to the best-fit relation shown as the solid line), though the scatter is large. This indicates that clumping is responsible for most of the remaining drop in luminosity, after accounting for changes in f_{hot}. The physical reason for the drop in C_{hot} is not obvious. One possibility is that larger systems are younger and hence less dynamically relaxed, and therefore contain more substruc-

ture. Another possibility is suggested by the analytic model of Bryan (2000), who also predicts a luminosity drop of a similar factor due solely to reduced "clumping" in smaller systems (compare his dot-dashed and solid lines in his Figure 3). In his case, this difference arises because cooling more efficiently removes hot gas in the central regions of smaller systems. As we will show in §4, we do not see a drop in the *mean* density in the inner regions of smaller systems, however the differences in C_{hot} do arise mainly in the inner regions. Regardless of cause, it is the combination of lowered subclumping and an overall drop in the hot fraction that is responsible for the lowered luminosities in smaller groups.

Figure 3 shows the relative impact of these two effects on the $L_X - T_X$ relation for groups in our simulation. We focus on $L_X - T_X$ here because its deviation from self-similarity is more evident than that of $L_X - \sigma_{\mathrm{DM}}$, at least above the break (cf. Figure 1). The solid points (at the bottom of the vertical lines) represent the groups reproduced from Figure 1. The open circles represent the group luminosities "corrected" to a common gas fraction and clumping factor,

$$L_{X,\mathrm{corrected}} = L_X (0.5/f_{\mathrm{hot}})^2 (C_{3 \ \mathrm{keV}}/C_{\mathrm{hot}}), \quad (3)$$

where f_{hot} is the fraction of hot baryons in each group, $C_{3 \ \mathrm{keV}}$ is the typical clumping factor for 3 keV groups, and C_{hot} is the clumping factor for the specific group (cf. Figure 2). If all groups had a hot fraction of 50% and a clumping factor of ≈ 20, this correction would have no effect. Instead, there is an increasingly larger correction for smaller systems. The solid portion of each vertical line represents the correction factor due to the mean hot fraction, and the dotted portion represents the remaining factor due to clumping. Figure 3 shows that the two effects are of comparable magnitude, and that the combination of the two brings the group luminosities into much better agreement with the self-similar relation (diagonal dotted line), though there is still some tendency for the lower mass groups to be underluminous. The best-fit relation for the "corrected" luminosities (which are not, of course, the physically predicted luminosities) has a slope of 2.4±0.2. The remaining discrepancy with the self-similar $L_X - T_X$ relation, and some of the remaining scatter, probably arise from the temperatures themselves, since
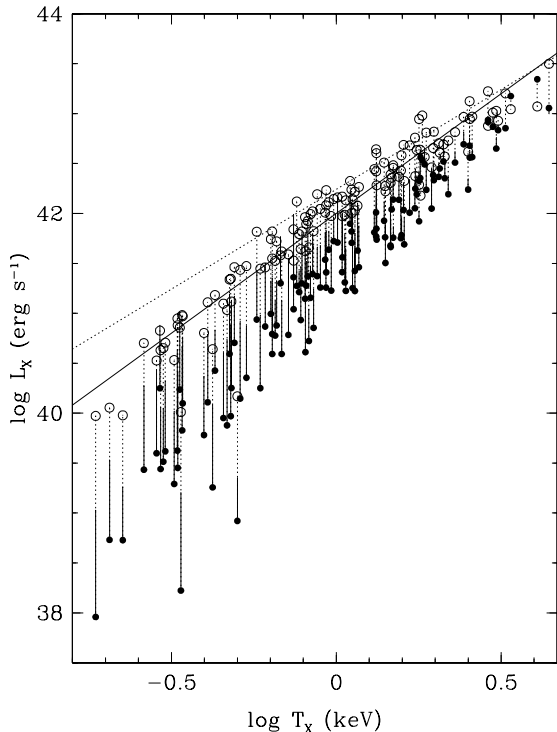
Fig. 3.— $L_X - T_X$ relation showing the relative importance of variations in mean hot gas density and clumping factor among our groups. The solid points are reproduced from Figure 1 (but not labeled by the number of member galaxies), while the open circles include correction factors to force all groups to have the same mean hot gas fraction and clumping factor (see eq. 3). Self-similar scaling is shown as the dotted line, and the best fit to the open circles is shown as the solid line, having a slope of 2.4 ± 0.2. The two portions of the vertical line segments represent the separate corrections due to hot gas fraction (solid) and clumping (dotted).

smaller groups tend to be hotter than the self-similar $T_X - \sigma$ relation predicts (see Figure 1).

A natural concern is that the clumping factor of our smaller groups is artificially suppressed by resolution effects, since our smallest systems contain as few as ~ 100 hot particles. Figure 4 shows a comparison of $L_X - \sigma_{\rm DM}$ from our high-resolution simulation (open circles) to the data shown in Figure 1 from our large-volume simulation (solid points). We focus on $L_X - \sigma_{\rm DM}$ because $\sigma_{\rm DM}$ is a more direct indicator of group mass than T_X. While the mass range probed by the two simulations is necessarily different, in the region of overlap they agree remarkably well. The best fit relation to the combined data is shown in the lower right, and is in good agreement with the scalings from Figure 1. If resolution were a major factor in the predicted departures from self-similar scaling, we would expect low mass groups to be systematically more luminous in the higher resolution simulation, and we would expect the break at $\sigma_{\rm DM} \approx 180$ km/s to shift down by a factor of two to $\sigma_{\rm DM} \approx 90$ km/s, corresponding to the factor of eight increase in mass resolution. While there is only one point well above the break from the high resolution simulation, it sits close to the mean $L_X - \sigma_{\rm DM}$ relation defined by the lower resolution, large-volume simulation. The good agreement in Figure 4 demonstrates that the reduced luminosity of low mass groups in our simulations is not an artifact of finite resolution but arises instead from the physical processes that the simulations incorporate. This test also indicates that our two-phase decoupling method for calculating luminosities is robust against modest changes in resolution.

In summary, the breaks in the $L_X - \sigma_{\rm DM}$ and $L_X - T_X$ relations are driven by the increased efficiency of radiative cooling in lower mass groups, which affects both the fraction and the density structure of the hot gas. The fraction of $T > 10^5$ K gas for our simulated groups drops from 50% at $\sigma \approx 500$ km/s to 20% at $\sigma \approx 100$ km/s, which explains the majority of the decline in luminosity relative to the self-similar prediction, while the remaining reduction is due to smaller systems having lower clumping factors $C_{\rm hot}$. This trend in hot fraction is consistent with observations, though the hot gas fractions of our large-volume simulation appear somewhat too low once surface brightness biases are taken into account. The hot gas
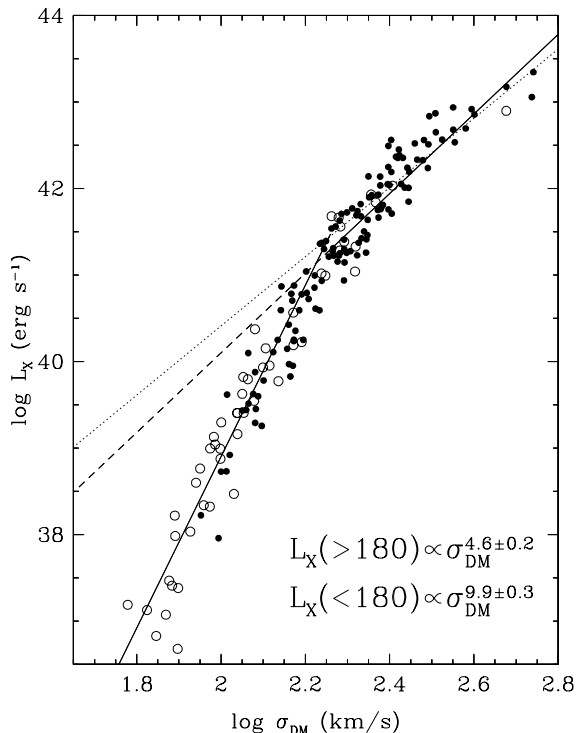
Fig. 4.— Resolution test of the $L_X - \sigma_{\mathrm{DM}}$ relation, showing the groups from the $(50h^{-1}\mathrm{Mpc})^3$ simulation (solid points, as in Figure 1 but not labeled by the number of member galaxies), and the higher resolution, $(22.22h^{-1}\mathrm{Mpc})^3$ simulation (open circles). The agreement in the region of overlap is very good, indicating that our results for the $L_X - \sigma_{\mathrm{DM}}$ relation are not significantly affected by numerical resolution. The scaling relations of the combined sample are shown as the solid line, and listed in the lower right. The dotted line shows self-similar scaling normalized to the largest systems.

fractions in our high-resolution simulation agree very well with observationally inferred values, and the $L_X - \sigma_{\mathrm{DM}}$ relations of the two simulations agree very well in their range of overlap.

The trend of a declining hot fraction in the group mass regime seems to be a generic feature of CDM-based galaxy formation, arising in hydrodynamic simulations of galaxy formation (Kay et al. 2000; Blanton et al. 2000; Pearce et al. 2001; this paper) and semi-analytic models (Bower et al. 2001). At the present epoch, the cooling time in the intragroup medium is long, but during the early stages of their assembly, a larger fraction of baryons were able to cool in smaller systems. This rather straightforward physical process just happens to become important in the mass regime of groups, and it results in a breaking of self-similarity in the observed scaling relations.

4. Profiles

Radial profiles of physical quantities such as temperature, surface brightness, and electron density can provide insights into galaxy formation processes within groups. In this section we present our simulation results for these profiles, fit beta models to the surface brightness profiles, and compare with observations, including the entropy-temperature relation derived in PCN99.

4.1. Average Profiles

Figure 5 shows the average surface brightness, temperature, electron density, entropy, and clumping factor profiles for our simulated groups, divided into four mass bins with 32 groups per bin. Profiles are scaled to the group Virial radius, then averaged. The surface brightness profiles (top panel) are shown scaled to the group central surface brightness. They are generally similar in form down to our smallest groups. This result contrasts with, e.g., Figure 1 of PCN99, where the surface brightness profile is significantly shallower for smaller systems. However, MZ98 find the shapes of surface brightness profiles for poor groups to be quite similar to those of clusters, consistent with our simulated profiles. We will examine these issues in more detail when we discuss beta models in the next section.

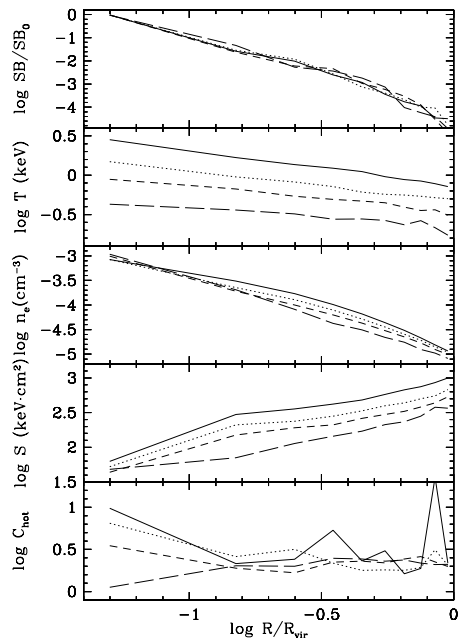Our temperature profiles (second panel) show a slight drop from the inner to outer parts. We

11

Fig. 5.— Radial profiles of surface brightness (top panel), temperature (second), electron density (third), entropy (fourth), and clumping factor (bottom) for the simulated groups, divided by mass into four equal number subsamples (solid, dotted, short-dashed, and long-dashed lines, from highest to lowest mass). The surface brightness and temperature profiles are projected, averaged in cylindrical shells, while the other profiles are 3-d, averaged in radial shells.

do not produce a cool central region often seen in groups (e.g., HP00) or cooling flow clusters (e.g., Allen, Schmidt, & Fabian 2001); we will return to this issue in §4.3. However, beyond the innermost regions, both group and cluster temperature profiles are observed to have a slight drop with radius (MZ98; HP00; de Grandi & Molendi 2002). In clusters, where one is able to probe almost out to the Virial radius, BeppoSAX observations by de Grandi & Molendi (2002) indicate an isothermal core (for non-cooling flow clusters) out to $0.2R_{\rm vir}$, and then a 30-40% drop out to $0.5R_{\rm vir}$, which they claim is a steeper drop than predicted by numerical simulations. From $0.2R_{\rm vir}$ to $0.5R_{\rm vir}$, our smallest groups show a 20% drop in temperature, while our larger groups show a 40% drop, consistent with their observations. Out to the Virial radius, the drop is around a factor of two. Thus, with minor discrepancies, our simulations generally reproduce observed temperature profiles outside of $0.2R_{\rm vir}$, predicting temperature profiles that are falling slowly towards large radius. We have presented projected temperature profiles in Figure 5 to allow more straightforward comparison to observations, but our conclusions from the 3-D profiles would not be significantly different.

The electron density profiles (middle panel) for the three subsamples would lie on top of each other in a purely self-similar model. The fact that smaller groups have lower n_e is a signature that cooling has operated more efficiently in these systems, as we showed in Figure 2. Figure 5 shows that cooling preferentially removes hot gas at intermediate radii. It is here that the cooling time is comparable to a Hubble time, and hence there is the most dramatic difference between large and small systems. In the central region, the cooling time has been short compared to a Hubble time over much of the group's life, while in the outskirts it is much longer than a Hubble time; thus in both regimes the electron density is similar across all groups. The shapes of our simulated density profiles are markedly different from those predicted in a pre-heating scenario, where the electron density profile would show an increasingly large core in smaller systems. Unfortunately there are no direct observations of the electron density profile, only estimates from beta-model fitting of surface brightness profiles (PCN99). The combination of rapidly improving Sunyaev-Zel'dovich and X-ray

12

observations of groups may yield electron density profiles in the future.

The entropy profile (second from bottom) is computed by taking the mass-averaged value of $T/n_e^{2/3}$ of all particles within each bin. The entropy profile declines smoothly from the outer edge into the center, in agreement with simulations by Thomas et al. (2002) and analytic expectations based on convective equilibrium (Voit et al. 2002), though they differ from those in the analytic model of Babul et al. (2002). We will discuss entropy further in §4.4.

The clumping factor profile (bottom panel) shows $\sum \rho_i / N_{\rm hot} \bar\rho_{\rm hot}$ (cf. eq. 2, but now the sum is over particles in each radial bin, and $N_{\rm hot}$ and $\bar\rho_{\rm hot}$ are the particle number and mean density of hot gas in the bin). The largest systems show a noisy profile in the outer parts, presumably because these objects are dynamically younger and have more subclumps due to recent merging. However, the systematic mass dependence of these profiles arises mainly at small radii, where larger systems show significantly more clumping. It is this inner region that drives the trend seen in the bottom panel of Figure 2, and consequently (a portion of) the luminosity drop in Figure 3. In part this trend arises because the largest systems often contain a single dominant galaxy in the center, whereas in smaller systems there can be significant offsets between the group center and the largest galaxy's position. The lower $C_{\rm hot}$ values at small radii in smaller groups do not appear to be resolution artifacts, since the luminosities predicted by the high-resolution and large-volume simulations agree (Figure 4) and the electron density profiles do not flatten in the centers of small groups, as would be expected if resolution effects were important.

In summary, profiles may have greater power to discriminate between models of group and cluster formation than scaling relations alone, since the latter can be adequately reproduced in both cooling and pre-heating models. In particular, the surface brightness profile appears to be a key diagnostic, with initial indications being that our simulations may be in disagreement with observations. We now examine this issue in more detail.

4.2. Beta Models

The canonical form for representing an X-ray surface brightness profile is a "beta model". In this model, the parameter β represents the ratio of the specific energy in dark matter to that of the hot gas, namely

$$\beta = \frac{\mu m_p \sigma^2}{k_B T}, \qquad (4)$$

where μ is the molecular weight and m_p is the proton mass. For an isothermal sphere in hydrostatic equilibrium with a King model density profile, the resulting surface brightness profile is

$$S(r) = S(0)\left(1 + r/r_{\rm core}\right)^{-3\beta + 0.5}, \qquad (5)$$

where $S(r)$ is the azimuthally averaged surface brightness at projected radius r, and $r_{\rm core}$ is the core radius. The electron density distribution also follows a similar form, with an exponent of $-3\beta/2$.

Observationally, β may be estimated either via equation (4), inferring the gas temperature from the X-ray spectrum and obtaining the velocity dispersion or mass independently, or via equation (5), by fitting surface brightness profiles. These spectroscopic and imaging estimates of β are usually referred to as $\beta_{\rm spec}$ and $\beta_{\rm fit}$, respectively. Unfortunately, the two estimates have historically yielded discrepant answers even in well-studied clusters, with $\beta_{\rm fit} \approx 2/3$ (Mohr, Mathiesen & Evrard 1999) and $\beta_{\rm spec} \approx 1$ (see discussion in Mulchaey 2000). Using hydrodynamic simulations, Navarro, Frenk, & White (1995) find that fitting surface brightness profiles yields $\beta_{\rm fit} \approx 0.8$ even when $\beta_{\rm spec} \approx 1$ because the dark matter mass profiles deviate systematically from a King model. Furthermore, they demonstrate that fitting to a smaller fraction of the Virial radius (as often done in observational analyses, especially of groups) biases $\beta_{\rm fit}$ even lower. These biases were invoked to reconcile observations of $\beta_{\rm spec}$ and $\beta_{\rm fit}$. However, recent *Chandra* observations of six large clusters with lensing masses suggest $\beta_{\rm spec} \approx 0.7$ (Allen, Schmidt, & Fabian 2001), so there may be no discrepancy to be explained after all.

Determinations of $\beta_{\rm fit}$ for groups are even more unsettled, primarily because only a small portion of the surface brightness profile is visible in these faint systems, and also because the contribution from a central galaxy, which is excluded

to obtain the intragroup gas properties, is typically more important than in clusters. HP00 find a median $\beta_{\rm fit} = 0.46$ from 24 groups with $T_X \approx 0.4 - 1.6$ keV. This implies considerably flatter surface brightness profiles than in clusters, a fact that is the basis for the "entropy floor" of PCN99. However, MZ98 find a median $\beta_{\rm fit} \approx 0.8$ for 9 groups, which is *higher* than typical observed values for clusters. Both MZ98 and HP00 use two-component beta models that are statistically warranted by the data, and in fact they consider many of the same groups. The fits of HP00 for groups in common with MZ98 yield much smaller core radii and smaller $\beta_{\rm fit}$, suggesting a strong degeneracy between $r_{\rm core}$ and $\beta_{\rm fit}$ (Mulchaey 2000). HP00 claim to see a trend for lower $\beta_{\rm fit}$ in smaller systems, but this could be an artifact of the bias mentioned above, where fits to a smaller fraction of the Virial radius yield lower $\beta_{\rm fit}$ values, since observations of their smallest groups extend to only $\sim 10-20\%$ of the Virial radius. Thus, in our view, the case for flatter surface brightness profiles in smaller groups has not been clearly proven.

Figure 6 shows a histogram of $\beta_{\rm fit}$ values from two-component beta model fits to our simulated group surface brightness profiles. The four line types correspond to our equal number subsamples. All groups with $\beta_{\rm fit} > 1.6$ are stacked in the rightmost bin. We allow the two components to simultaneously vary freely in our Marquardt minimization routine, then take the β value associated with the component having the larger $r_{\rm core}$, since it presumably represents the intragroup component[4]. The median values of $\beta_{\rm fit}$ and $r_{\rm core}$ are 0.66 and $0.2R_{\rm vir}$, respectively. The second component (not shown) has median $\beta_{\rm fit} \approx 0.5$ and $r_{\rm core} \approx 0.03R_{\rm vir}$.

Our median $\beta_{\rm fit} = 0.66$ is intermediate between that of HP00 and MZ98. We find only a slight trend with size: our subset of largest groups has a median $\beta_{\rm fit} = 0.68$, while our subset of smallest groups has median $\beta_{\rm fit} = 0.62$. We find that for many groups, the two-component beta model is not a good fit even though sensible values of $\beta_{\rm fit}$ are returned. Since groups are not strictly

---

[4]In the case of groups, where the central galaxy may make a significant contribution to the gravitational potential, we are not convinced that it is sensible to fit the "galaxy" as a physically distinct component, but here we follow the standard practice of observational analyses.
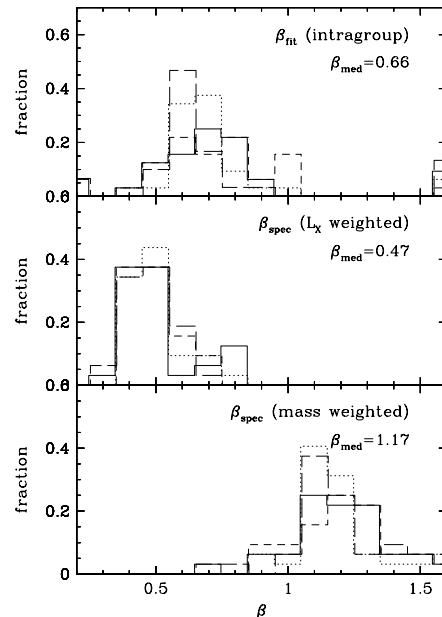

Fig. 6.— *Top panel:* Histogram of $\beta_{\rm fit}$ for the intragroup surface brightness component of two-component beta models fit to our groups. Median $\beta_{\rm fit}$ value is indicated in upper right. *Middle panel:* Histogram of $\beta_{\rm spec}$ for luminosity-weighted group temperatures. *Bottom panel:* Histogram of $\beta_{\rm spec}$ for mass-weighted average group temperature. In each panel, the four histograms correspond to four mass bins containing nearly equal numbers of groups, with solid, dotted, short-dashed, and long-dashed lines in decreasing order of mass.

isothermal, do not follow King model profiles, and are typically not spherically symmetric (especially smaller systems), perhaps this result is not surprising. It may, however, explain why the observed fits are so sensitive to the details of the fitting procedures. Further evidence that beta models are inappropriate comes from a comparison of the surface brightness and electron density profiles in Figure 5; though the former have a similar shape across all systems, the latter do not.

In principle, surface brightness profiles offer an excellent diagnostic of intragroup gas physics. Unfortunately, current observational determinations of $\beta_{\rm fit}$ appear too uncertain to validate or invalidate any models. This situation is likely to change with *XMM* and *Chandra*, given their increase in sensitivity and spatial resolution. If observations of flatter surface brightness profiles in smaller groups persist (i.e., if $\beta_{\rm fit}$ correlates with temperature), they would pose a serious challenge for our simulation predictions. Similar values of $\beta_{\rm fit}$ in groups and clusters, on the other hand, would strongly favor the scenario presented here, in which cooling rather than pre-heating is the primary cause of deviations from self-similar scaling. Directly measured profiles will be more informative than model fits, since beta models implicitly incorporate a number of assumptions that may not be true in detail.

4.3. Group Temperatures and $\beta_{\rm spec}$

The middle and bottom panels of Figure 6 show histograms of $\beta_{\rm spec}$ from our simulated groups. The middle panel shows $\beta_{\rm spec}$ when the usual luminosity-weighted temperature is used, and the bottom panel shows the case when the mass-weighted temperature is used; in both cases we have used $\sigma_{\rm DM}$ for the velocity dispersion. Interestingly, the luminosity-weighted case shows significant deviations from the expected $\beta = 1$, with a median value of $\beta_{\rm spec} = 0.47$. Thus, the luminosity-weighted temperatures are roughly twice the groups' Virial temperatures. Conversely, the mass-weighted temperatures underestimate the Virial temperature by $\sim 20\%$. There is no systematic trend of $\beta_{\rm spec}$ with group mass in either case.

Adiabatic simulations yield $\beta_{\rm spec} \approx 1$ (e.g. Navarro, Frenk, & White 1995). As emphasized by Allen, Schmidt, & Fabian (2001), this value

appears high compared to the latest *Chandra* observations of clusters, where $\beta_{\rm spec} \approx 0.7$. Hints of this discrepancy were already present in earlier ROSAT data (see Thomas et al. 2002, for a summary). In the simulations of Thomas et al. (2002), either cooling or pre-heating produces increased temperatures compared to the adiabatic case, yielding better agreement with the data. With pre-heating, the reason for the increased temperature is obvious, but in the case of cooling, this nonintuitive result arises because gas is cooled out of the center of the cluster, and the lowered pressure support draws in hotter gas from the outskirts (Pearce et al. 2000). The cluster simulation with cooling by Lewis et al. (2000) produced a similar result. In both cases, however, the derived value of $\beta_{\rm spec}$ was consistent with the latest observations, while our groups still appear too hot.

We conclude that our predicted luminosity-weighted temperatures are somewhat at odds with observations. We investigated whether the procedure of fitting Raymond-Smith models to coarsely binned X-ray spectra yielded some systematic temperature bias, and found that when groups have a temperature gradient towards the center (as in our larger systems), the fitted temperature underestimates the true luminosity-weighted temperature. However, the magnitude of this effect is quite small ($\sim 10\%$), and in any case it cannot explain the discrepancy in our smaller groups, which are nearly isothermal.

Instead, we believe the source of the discrepancy lies in the temperature profiles of our simulated groups (cf. Figure 5). In the sample of HP00, about half the groups show a clear drop in temperature, by as much as a factor of two, within $\sim 10-20\%$ of the Virial radius, and the majority of remaining groups are at least consistent with having a cooler central region. Similar results are seen in large clusters, though the drop in temperature is seen out to a smaller fraction of the Virial radius (Allen, Schmidt, & Fabian 2001). Our simulated groups, however, show no such drop, and since the emission is dominated by the central region, this leads to a much higher luminosity-weighted temperature. If we alter the temperatures of simulated group particles "by hand" so that they are lower in the center by an amount consistent with observations, then our median $\beta_{\rm spec}$ increases to

roughly 0.8, in agreement with observed values. (Specifically, we apply a linear temperature gradient such that the central temperature is half that at $0.2R_{\rm vir}$.)

It is not clear why our simulated groups do not have a cool central region, while observed groups do. If the physical process(es) that produce such a region are analogous to those in clusters, then the insights gained from recent cluster studies may provide clues. For instance, recent observations of cooling flow clusters suggest local isothermality in the central region (Boehringer et al. 2001a), with little emission from the cold component (Peterson et al. 2001), in conflict with the standard cooling flow model (Fabian 1994). These findings suggest that some unidentified heat source must counteract the cooling process, and serve to maintain the central gas in a quasi-static, slightly cooler state. This heat source may be AGN in the central galaxy (Boehringer et al. 2001b), heat conduction from the outer region (Narayan & Medvedev 2001), outflow induced shocks that can be seen in recent Chandra images, or some as yet undiscovered process. For instance, AGN are observed to produce "bubbles" in the intracluster medium, the walls of which contain denser, cooler gas (Nulsen et al. 2002); any emission weighted measure of temperature will be biased low by this gas since the emission depends on the density squared. If this or similar processes are operating in the centers of groups (at a proportionally reduced amplitude that would make them difficult to detect directly), then our simulations would be missing the input physics required to properly model the central regions in these systems. Alternatively, we note that the outer radius of the cool region is roughly the radius at which the metal-line cooling rate becomes smaller than a Hubble time (while with only the primordial cooling assumed in our simulation, the cooling time is still much longer). Hence it is possible that including metal-line cooling in our simulation would result in a cooler center, particularly if there is a metallicity gradient towards the center. However, as noted earlier, increased cooling does not necessarily reduce gas temperatures, since reduced central pressures allow hotter gas to flow in from the surrounding regions and experience adiabatic heating along the way.

4.4. Entropy

Entropy is a powerful diagnostic of intragroup gas, with a closer connection than temperature or density alone to the processes that determine its physical state (Bower 1997; Voit et al. 2002). The fact that groups appear to show excess entropy relative to that predicted purely from gravitational shock heating (PCN99) has been used to argue for the presence of non-gravitational heating processes, since radiative cooling reduces rather than increases gas entropy. However, a more complete analysis suggests that cooling can effectively raise the entropy inferred from X-ray data because the gas that cools onto galaxies is no longer observable in the X-rays at all; more efficient cooling in smaller systems can therefore produce an apparent "floor" in group entropies (C. Norman 2000, private comm.; Voit & Bryan 2001).

Figure 7 plots the entropy at 10% of the Virial radius against group X-ray temperature, for the simulated groups and the observational analysis of PCN99. The group entropy profiles (Figure 5) are reasonably well described by power laws. We compute entropies for Figure 7 by fitting each group's profile with a power law, then taking the value of the fit at $R = 0.1R_{\rm vir}$. The solid line shows the self-similar entropy relation derived using adiabatic simulations (see PCN99), $S(0.1R_{\rm vir}) = 45(T/{\rm keV})(f_{\rm gas}/0.06)^{-2/3}h^{-4/3}{\rm keV\ cm}^{-2}$, with $f_{\rm gas} = \Omega_b/\Omega_m = 0.118$ in our case.

It is clear that the simulated group entropies do not follow the self-similar relation, and are instead in reasonable agreement with the data (given their large error bars). This agreement is somewhat surprising given that our surface brightness profiles do not show the strong mass dependence inferred by PCN99, and it once again suggests that the canonical beta model may not be an appropriate description of poor groups. Our results are also in agreement with the analytic model of Bryan (2000), which is based on a declining hot fraction with group mass similar to that predicted by our simulation. Thus, it appears that the physical mechanism of cooling out low-entropy gas and leaving an effective "entropy floor" (Voit et al. 2002) is operating in our simulations. Note, however, that the simulation does not indicate a hard floor at $\sim 100\ {\rm keV\ cm}^2$, but rather a decline of entropy with group temperature that is slower than
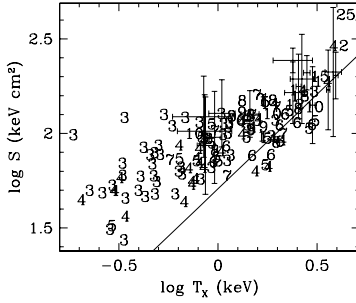
predicted by self-similar models.

5. Modeling Observed Systems

In the real universe, it is not possible to directly observe the luminosity, temperature, and dark matter velocity dispersion of a zero-metallicity intragroup medium out to the Virial radius. Hence, to compare theoretical predictions to observations, we must model observational effects in our simulations. In this section we consider some "real-world" effects and assess how they affect the inferred scaling relations and derived interpretations. Our analysis here is simple and intended only to indicate the sign and rough magnitude of such effects; we defer a detailed side-by-side comparison of simulated and observed groups to future work. We will see that there are non-trivial differences between the scaling relations of "observed" groups and the idealized ones discussed in §3, but that none of our fundamental conclusions are altered as a result.

5.1. Metallicity

Since metal lines provide a dominant contribution to the total luminosity at temperatures below a few keV, they could in principle significantly affect the predicted luminosity scaling relations. We include metals via a fit to the metallicity vs. temperature data in Figure 1 of Davis, Mulchaey, & Mushotzky (1999), namely

$$\log Z = 1.04 \log T_X - 0.73, \qquad (6)$$

where Z is the metallicity in solar units, and T_X is in keV. We cap the metallicity at the cluster value of 0.3 solar; systems above 1.6 keV are thus set to this metallicity. Note that Davis, Mulchaey, & Mushotzky (1999) derive a much steeper dependence of abundance on temperature for systems with $T_X < 1.5$ keV ($Z \propto T^{2.5}$). However this relation would produce unrealistically low metallicities for our smallest groups, so instead we use our fit to their entire data set up to $T_X \approx 3$ keV. While there has been some controversy regarding metallicities derived from *ASCA* data (see, e.g., Buote 2000), the low metallicities in the Davis, Mulchaey, & Mushotzky (1999) sample have now been confirmed in several cases with improved data from *XMM* (Mulchaey, private comm.). Thus, the drop in metallicity below
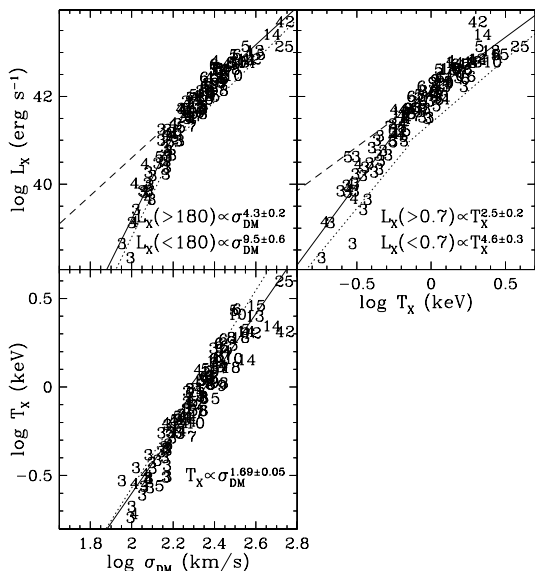

Fig. 7.— Entropy at $0.1R_{\rm vir}$ vs. X-ray temperature of simulated groups. The solid line shows the self-similar prediction, and the data points are taken from PCN99.

2 keV appears to be real, though it is not straightforward to explain (Mulchaey 2000).

Figure 8 shows our predicted scaling relations after incorporating equation (6) into our calculations with the Raymond-Smith code. The relations continue to show the same qualitative behavior, and the break values are not changed significantly. The luminosity relations are shallower above the break, since the metallicity is mostly constant in these larger systems, and metal lines provide a greater contribution in smaller (cooler) groups. Below the break, the relations are steepened because the metallicity is dropping with group mass. At 1 keV, the luminosity is higher by a factor ~ 3 compared to the zero-metallicity case (compare the dotted and solid lines in the luminosity relations), indicating the dominant contribution of line emission. The $T_X - \sigma_{DM}$ relation is also slightly affected, as higher mass systems have lower luminosity-weighted temperatures; this is because the relative luminosity weighting of low-temperature gas in the system increases with the presence of metals in this temperature regime. However, these small differences do not qualitatively affect our conclusions drawn from the zero-metallicity case (Figure 1).

While it appears that the metallicity in groups is lower than in clusters, this difference is not well established. We therefore test another model using a constant metallicity of $0.3Z_\odot$ in all groups, and we list the resulting scalings in Table 1. This calculation shows that if the metallicity is similar in groups and clusters, then the $L_X - \sigma_{DM}$ and $L_X - T_X$ slopes are shallower in all regimes. Even in this case, however, the breaks in the luminosity scalings remain quite evident.

5.2. Surface Brightness Effects

While current cluster observations can reach the Virial radius and sometimes beyond, this is rare in groups (Mulchaey 2000). Thus, group observations only probe the innermost regions, and it is not straightforward to compare their properties with clusters where physical quantities are measured over the entire system. We investigated how this difference affects derived baryon fractions in §3.2, and we now consider its effect on scaling relations.
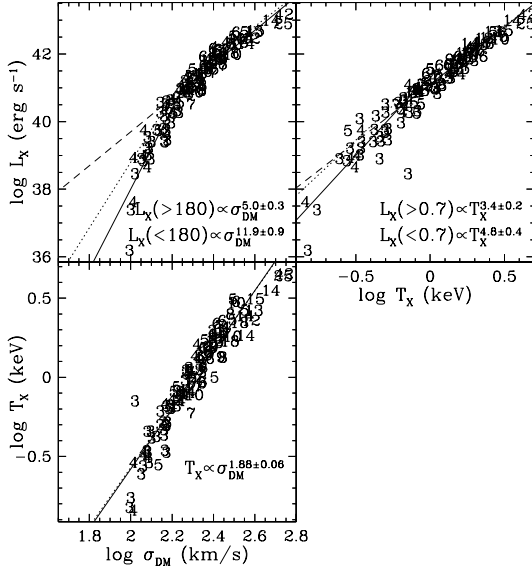
Figure 9 shows the result of applying the surface

Fig. 8.— Scaling relations as in Figure 1, but the X-ray luminosities and temperatures have been computed using a metallicity given by equation (6). The best-fit relations from Figure 1 have been reproduced here as the dotted lines.

Fig. 9.— Scaling relations as in Figure 1, but the X-ray luminosities and temperatures have been computed only out to an "observable" fraction of the Virial radius as given by equation (1). These calculations assume zero metallicity. The best-fit relations from Figure 1 have been reproduced here as the dotted lines.

brightness cut in equation (1) to our groups. Note that we have reset the metallicity to zero to isolate the effects. Comparing to Figure 1 (whose best-fit scalings are reproduced as the dotted lines), the luminosity relations are somewhat steeper, as is expected since the surface brightness cut is stronger in smaller systems. But the effect is fairly mild, even in small groups where the fraction of the Virial radius probed is 20% or less. The $T_X - \sigma_{\rm DM}$ relation is essentially unaffected.

The reason that the surface brightness cut has only a mild effect is that most of the group luminosity comes from the central region (cf. Figure 5), so there is minimal impact until the cut-off radius becomes a fairly small fraction of the Virial radius. Still, one must be cautious about interpreting observations where less than 20% of the group's Virial radius is being probed, especially because the scatter in X-ray surface brightness between groups will select out the brightest groups of a given mass. Note that we did not include scatter in the X-ray extent relation used in equation (1), whereas observations show a sizeable scatter (Mulchaey 2000). Overall, however, current observations are sensitive enough to probe scaling relations down to fairly small groups reasonably reliably, assuming that issues of point-source contamination and Galactic foreground can be overcome.

5.3. Velocity Dispersion Bias

In computing $L_X - \sigma$ and $T_X - \sigma$ relations in §3, we have used the dark matter velocity dispersion $\sigma_{\rm DM}$. However, the observed velocity dispersion is typically computed from galaxies, which may be biased relative to the dark matter, and this can influence the interpretation of the observed correlations. In this section we examine this bias and its effect on the observed scaling relations.

The top panel of Figure 10 shows the group mass vs. $\sigma_{\rm DM}$. There is a very tight correlation, as would be expected for relaxed systems. As before, the plot symbols indicate the number of galaxies in each group. The bottom panel shows the ratio of the galaxy velocity dispersion $\sigma_{\rm gal}$ to $\sigma_{\rm DM}$, where

$$\sigma_{\rm gal}^2 = \frac{1}{N_{\rm gal}-1} \sum_{i=1}^{N_{\rm gal}} |\mathbf{v}_{{\rm gal},i} - \langle \mathbf{v}_{\rm gal} \rangle|^2 , \quad (7)$$

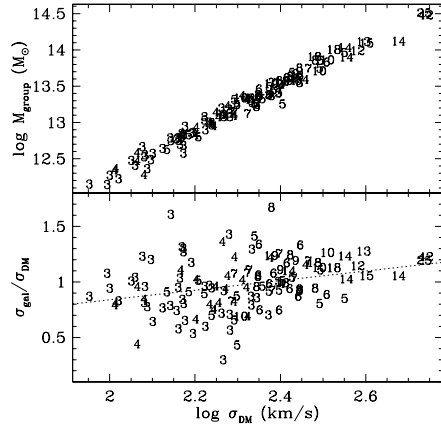and $\langle \mathbf{v}_{\rm gal} \rangle$ is the (unweighted) mean velocity of the

Fig. 10.— *Top panel:* Group mass vs. dark matter velocity dispersion. *Bottom panel:* Ratio of velocity dispersion calculated from galaxies to that of the dark matter. The dotted line shows a linear fit to the data points.

galaxies. There is a weak but discernible trend for smaller systems to have their velocity dispersion underestimated. The dotted line shows the best fit linear relation, which suggests that on average, at $\sigma_{\rm DM} = 100$ km/s, the galaxy velocity dispersion underestimates the true velocity dispersion by 15%. Conversely, the galaxy velocity dispersion of large groups is slightly higher than $\sigma_{\rm DM}$ on average. Moreover, there is an increasing scatter to smaller systems, since there are only a few galaxy tracers with which to estimate the dispersion. This scatter could be larger still in observational studies because of projection effects (Tovmassian, Yam, & Tiersch 2002). Hence, using galaxy velocity dispersions, particularly in systems with few identified members, may have an impact on the velocity dispersion scaling relations.

Figure 11 shows the simulated group scaling relations $L_X - \sigma_{\rm gal}$ and $T_X - \sigma_{\rm gal}$. $L_X - T_X$ is not shown since it is (obviously) unchanged from Figure 1. The velocity dispersion scalings, on the other hand, are substantially altered. $L_X - \sigma_{\rm gal}$ shows a somewhat shallower slope consistent with self-similarity, and the fitted slope below the previous break value of 180 km/s is now identical to the slope above it. Meanwhile, $T_X - \sigma_{\rm gal}$ shows a relation much shallower than obtained using $\sigma_{\rm DM}$, with $T_X \propto \sigma_{\rm gal}^{1.13}$.

To examine this result in greater detail, we selected the eleven simulated groups that have ten or more member galaxies, then took a subset of the $N_{\rm gal}$ most massive galaxies in each group and recomputed $\sigma_{\rm gal}$. In Figure 12, points with solid error bars show the mean and the 1-σ scatter of the ratio $\sigma_{\rm gal}/\sigma_{\rm DM}$ as a function of the number of galaxies $N_{\rm gal}$ used in the $\sigma_{\rm gal}$ calculation. At high $N_{\rm gal}$, the ratio is close to unity and the scatter is small, but for low $N_{\rm gal}$ the scatter is large and the mean is biased low. If we exclude the most massive galaxy from the velocity dispersion calculation (points with dotted error bars), then the mean ratio remains close to unity even at low $N_{\rm gal}$, which demonstrates that the bias in $\sigma_{\rm gal}$ arises mainly from the tendency of the most massive, central galaxy to move slowly with respect to the group center-of-mass velocity. However, if we recalculate the $T_X - \sigma_{\rm gal}$ relation using velocity dispersions that exclude the most massive galaxy, we still get a fitted slope of ≈ 1.1. This demonstrates that it is the *random scatter* in the galaxy velocity dis-
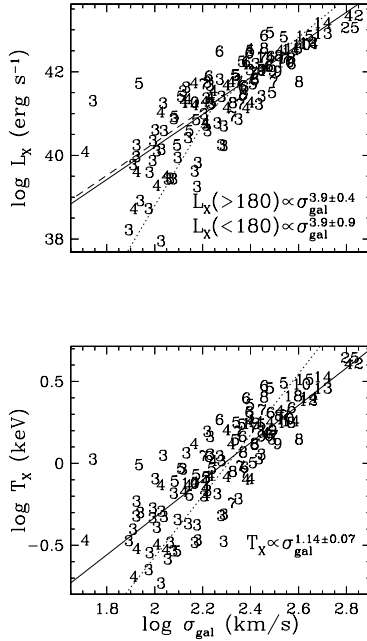
Fig. 11.— Velocity dispersion scaling relations with the velocity dispersion computed from the galaxies rather than the dark matter. The best-fit relations from Figure 1 are shown as the dotted lines.

person estimates that affects the $T_X - \sigma_{\mathrm{gal}}$ slope, not the small *systematic* bias of σ_{gal} with respect to σ_{DM}. Our fits to $L_X - \sigma_{\mathrm{gal}}$ and $T_X - \sigma_{\mathrm{gal}}$ are performed in log space without accounting for random errors in the estimation of the true σ from σ_{gal}. Since downward fluctuations reduce $\log \sigma$ more than upward fluctuations increase it, the effect of these random errors is to flatten the $L_X - \sigma$ and $T_X - \sigma$ relations, especially in the low mass regime where the errors are larger.

Noisy velocity dispersion estimates may explain some conflicting observational results regarding the $T_X - \sigma$ relation. HP00 find $T_X \propto \sigma_{\mathrm{gal}}^{0.9}$, and they interpret the higher-than-expected temperatures at low σ_{gal} as evidence for pre-heating. However, the velocity dispersions of their smallest groups were typically computed from 3–5 member galaxies (compiled from the literature). It is not strictly fair to compare their slope with our $T_X - \sigma_{\mathrm{gal}}$ slope, since our galaxy samples have different "completeness limits", but it is illustrative that the slopes are similar. Conversely, the MZ98 sample includes only groups with over 20 spectroscopic members, and they find $T_X \propto \sigma_{\mathrm{gal}}^{2.2 \pm 0.9}$, in agreement with cluster samples.

In the currently relevant observational regime ($\sigma \gtrsim 200$ km/s), the $L_X - \sigma$ relation is not significantly affected by the scatter in σ_{gal} (Figure 11, top). HP00 find $L_X \propto \sigma_{\mathrm{gal}}^{4.4}$, consistent with self-similarity, but they attribute this to coincidentally canceling reductions in L_X owing to pre-heating, and in σ_{gal} owing to a noisy estimation from a small number of galaxies. Our analysis shows that, at least for groups of this size, the $L_X - \sigma_{\mathrm{gal}}$ relation is unaffected within current observational errors. In support of this idea, MZ98 and Zimer, Zabludoff & Mulchaey (2001) also find $L_X \propto \sigma_{\mathrm{gal}}^{4.3-4.4}$ using many more galaxies per group. Tovmassian, Yam, & Tiersch (2002) argue that the velocity dispersion bias arises because of geometrical projection effects in 1-D dispersion estimates, and they also find $L_X \propto \sigma_{\mathrm{gal}}^4$ when properly accounting for such effects.

In summary, velocity dispersion bias can have a significant effect on the $T_X - \sigma$ relation, but only a mild effect on $L_X - \sigma$, at least above the break. Observations that have sufficient numbers of galaxies per group ($\gtrsim 10$) indicate little evidence for the anomalously hot intragroup gas in poor groups that would be expected in a pre-
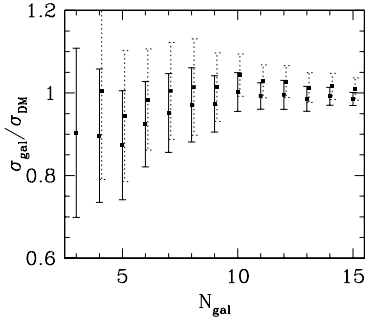
5.4. Comparison to Observations

Though there are still many fundamental differences between the way our simulations and observations are analyzed, as well as some inherent modeling difficulties in our simulation, it is nevertheless instructive to compare our scaling relation predictions with available observations. To model observations as closely as we can given current constraints, we apply the metallicity relation as in equation (6), we include surface brightness effects as in equation (1), and we use the dark matter velocity dispersion. The last choice is motivated by the fact that the latest group samples have deep imaging that permits identification of 10-50 group members (e.g. Zimer, Zabludoff & Mulchaey 2001), which should be sufficient to trace the true mass of the group much like σ_{DM}, though still with somewhat larger scatter.

Figure 13 shows the resulting scaling relations, and the fits are also listed in Table 1. The $L_X - \sigma_{\mathrm{DM}}$ relation slopes above and below the break are close to those in a compilation of clusters, groups and galaxies by Mahdavi & Geller (2001), who found $L_X \propto \sigma^{4.4}$ down to $\sigma = 350$ km/s and $L_X \propto \sigma^{10}$ below that down to galaxy scales. Our break occurs at a lower σ than theirs, but the observed relation is poorly constrained in the break region, and the data sample is inhomogeneous, so the discrepancy may not be too serious.

The slope of the $L_X - T_X$ relation above the break is in good agreement with MZ98 and Zimer, Zabludoff & Mulchaey (2001), and it is also consistent with the observed relation in clusters (White, Jones, & Forman 1997). However, it is in poor agreement with samples by HP00 and Xue & Wu (2000), who find $L_X \propto T_X^{4.9}$ and $L_X \propto T_X^{5.6}$. Those results are in better agreement with the slope *below* our break at 0.8 keV. These samples have $T_X \approx 0.4 - 1.6$ keV, thus their steep slopes suggest a higher break temperature, perhaps $\sim 1 - 1.5$ keV. As with our $L_X - \sigma$ relation, our break appears to occur at a mass that is slightly too low.

Our $T_X - \sigma$ relation shows some deviation from self-similarity ($T_X \propto \sigma^{1.75}$), although as we saw in §5.1, this deviation arises mostly from metal line emission weighted into the temperature de-

Fig. 12.— Velocity dispersion calculated from the N_{gal} most massive galaxies within a group, divided by the velocity dispersion of the dark matter. Points with solid error bars show the calculation using equation (7), while points with dotted error bars indicate the effect of excluding the most massive galaxy before computing σ_{gal}. Results are computed only for the 11 simulated groups that have ten or more member galaxies. The error bars represent the $1 - \sigma$ scatter of σ_{gal} values within each bin; the error on the mean of $\sigma_{\mathrm{gal}}/\sigma_{\mathrm{DM}}$ is smaller (e.g., for points at $N_{\mathrm{gal}} \leq 10$, it is lower by a factor of $\sqrt{11}$).
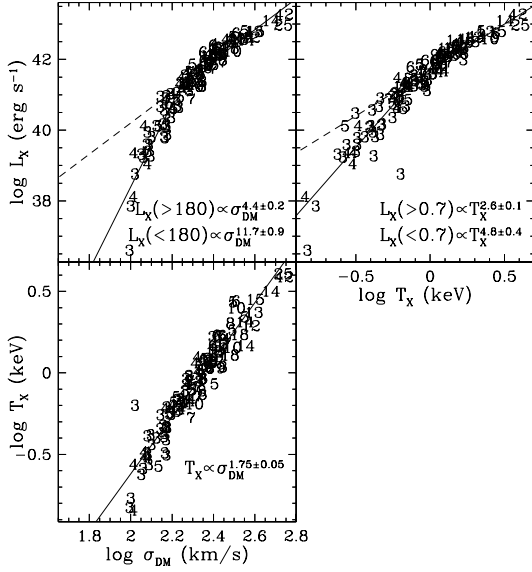
Fig. 13.— Scaling relations as in Figure 1, but the X-ray luminosities and temperatures have been computed using a metallicity given by equation (6) and a surface brightness cut given by equation (1). This represents our attempt to most closely match current observations, which are discussed in the text.

termination, not from any physical process that actually raises the gas temperature. Metal line cooling is another way in which the $T_X - \sigma$ relation can mimic excess temperature in $T_X \lesssim 1$ keV groups, in addition to the effects of scatter in σ estimates from small numbers of galaxies (§5.3). Observations suggest that the $T_X - \sigma$ relation is fairly close to self-similar from clusters down to groups (Mulchaey 2000), in agreement with our predictions.

So far we have not discussed the amplitudes of the various scaling relations, only the slopes. Our $L_X - \sigma$ relations amplitude is in very good agreement with observations. MZ98, HP00, and Zimer, Zabludoff & Mulchaey (2001) all find $L_X = 10^{42.5}-10^{42.7}$erg s^{-1} at $\sigma = 300$ km/s where the observations are relatively reliable, while we obtain $L_X = 10^{42.5}$erg s^{-1}. This is encouraging, given that this (large-volume) simulation cools an excessive fraction of baryons (see Figure 2 and the accompanying discussion), and we have made large corrections to the luminosities based upon our two-phase decoupling (see §2). If our predictions were highly sensitive to these effects, it would be quite a coincidence that they conspired to bring our luminosity-mass relation into such good agreement with observations.

Conversely, the amplitudes of the temperature relations are in poor agreement with observations. As discussed in §4.3, our luminosity-weighted temperatures are higher than observed by a factor of $\approx 1.5 - 2$ at a given σ. The lower factor comes from considering $\beta_{\rm spec}$ as observed in *Chandra* data of large clusters by Allen, Schmidt, & Fabian (2001) (with the caveat that our systems are much smaller than any observed by those authors); the higher factor comes from comparing the amplitude of our $T_X - \sigma$ relation with *ROSAT* observations. For example, we predict a temperature of 1.7 keV at $\sigma = 300$ km/s, while MZ98 and HP00 find 0.8 and 0.9 keV, respectively, for such systems. It remains to be seen whether *Chandra* observations of these groups will yield higher temperatures as has happened for some clusters.

In the $L_X - T_X$ relation, this overestimation of temperatures translates to our predicted luminosities being too low by a factor $\sim 3 - 8$ at fixed T_X (for $L_X \propto T_X^3$). For example, at $T_X = 1$ keV, MZ98 find $L_X = 10^{42.4}$erg s^{-1}, HP00 find $L_X = 10^{43}$erg s^{-1}, and the extrapolation of

the White, Jones, & Forman (1997) relation yields $L_X = 10^{42.7}$erg s^{-1}; our simulated groups yield $L_X = 10^{41.7}$erg s^{-1} at this temperature. As discussed in §4.3, the *ad hoc* correction of lowering the temperature of gas within $0.2R_{\rm vir}$ in accordance with temperature profiles seen by HP00 results in lowering our groups' T_X by ~70%, and such a reduction (regardless of what physical phenomenon is responsible for it) brings both our $T_X - \sigma$ and $L_X - T_X$ relations into the observed range.

In summary, our simulation seems to do a good job of reproducing the slopes of observed scaling relations, but the breaks in the $L_X - \sigma$ and $L_X - T_X$ relations appear to occur at a group mass that is somewhat too small. This discrepancy might be resolved by improvements in the numerics or astrophysical modeling, or it could indicate that some degree of pre-heating is still required, though much less than in a model with adiabatic gas dynamics. The amplitude of our $L_X - \sigma$ relation agrees reasonably well with observations, suggesting that our groups' luminosities are being accurately modeled. However, our simulated X-ray temperatures appear to be discrepant with observations, being too high by a factor of $1.5 - 2$ at a given mass. This discrepancy manifests itself in both the $L_X - T_X$ relation and the $T_X - \sigma$ relation. The lower temperatures of observed groups appear to be connected to cooler central regions that are not reproduced by our simulation. We suspect that the cause of this discrepancy is astrophysical, perhaps our use of zero-metallicity cooling curves during dynamical evolution, or perhaps the absence of a significant physical process such as AGN heating or conduction.

6. Conclusions

Using a large-scale hydrodynamic cosmological simulation that is able to resolve sub-$L_\star$ galaxies, we have investigated the X-ray scaling relations for galaxy groups with velocity dispersions ranging from $100 - 550$ km/s. In particular, our goal was to assess whether these scaling relations are consistent with those predicted by simple self-similar models and adiabatic simulations. Our main findings are:

1. Our luminosity scaling relations $L_X - T_X$ and $L_X - \sigma$ do not follow the self-similar form at any point in our mass range. The simulated relations are always steeper than the self-similar predictions, with lower luminosities at smaller masses.

2. These scaling relations show a "break" around 180 km/s (0.7 keV), below which the relations steepen even further.

3. The $T_X - \sigma$ relation shows no break, and its slope is reasonably consistent with the self-similar model, indicating that these groups are Virialized and in hydrostatic equilibrium.

4. In our simulations, self-similarity is broken mainly as a result of the hot gas fraction falling with group size, from $\approx 50\%$ of the baryonic mass at $\sigma = 500$ km/s to $\approx 20\%$ at $\sigma = 100$ km/s. There is a secondary effect from the fact that the hot gas clumping factor (mostly in the groups' central regions) drops by a factor of roughly three over this mass range.

5. Our large-volume simulation cools too many baryons, resulting in a typical hot fraction that is lower than observed by $\sim 40\%$, once X-ray surface brightness thresholds are taken into account. Our high-resolution simulation predicts *more* hot gas at a given group mass, and is in good agreement with observations. Thus, the amplitude of the $f_{\rm hot} - \sigma$ relation is somewhat sensitive to resolution, though not in the sense that one might naively expect. The *trend* of falling hot gas fraction towards lower group mass, which arises in both simulations and accounts for most of the departure from self-similar scaling relations, is consistent with available observations.

6. Our two simulations, which differ in mass resolution by a factor of eight, predict very similar X-ray luminosities at fixed group mass. To the extent that we can test them with these simulations, the departures of the $L_X - \sigma$ and $T_X - \sigma$ relations from self-similar scaling are not artifacts of numerical resolution: the reduced luminosities of low mass groups are a result of physical processes that are modeled consistently between the two simulations.

7. Surface brightness profiles offer an excellent diagnostic for constraining gas physics in groups, in particular for distinguishing cooling from pre-heating as the primary cause of departure from self-similar scalings, but current observations are too uncertain to give clear guidance. Our groups' median $\beta_{\mathrm{fit}} = 0.64$ is intermediate between various observations, and we predict no significant trend of β_{fit} with group size. Our simulations do reproduce the observed entropy-temperature relation (PCN99), though we do not predict a hard floor but merely a shallower decline of entropy with group mass than predicted in self-similar models.

8. Accounting for the effects of metallicity or for observational biases due to X-ray surface brightness thresholds does not qualitatively alter the conclusions listed above.

9. Noisy estimates of group velocity dispersions have a significant effect on the derived $T_X - \sigma$ relation. The most massive galaxy in a group tends to move close to the group center-of-mass velocity, so its inclusion in a velocity dispersion estimate biases σ low when the number of galaxies is small. Even more important is the scatter in σ when the number of tracers is small, which biases a simple fit of $T_X - \sigma$. Our simulations suggest that $\gtrsim 10$ galaxies are needed to obtain velocity dispersions that are precise enough for $T_X - \sigma$ determination. Noisy σ estimates may account for some of the discrepancies between apparently conflicting observational analyses. The $L_X - \sigma$ relation can also be biased by noisy σ estimates, but this effect does not seem to be important in the mass range probed by current data.

10. Accounting for observational biases, our scaling relation slopes are roughly in agreement with observations, though our break appears at somewhat too low a group mass. With our best attempts to mimic current observational approaches, our simulation predicts the following scaling relations for galaxy groups with $\sigma \lesssim 500$ km/s:

   - $L_X \propto \sigma^{4.4}$ for $\sigma > 180$ km/s, and
     $L_X \propto \sigma^{11.7}$ for $\sigma < 180$ km/s.

   - $L_X \propto T_X^{2.6}$ for $T_X > 0.7$ keV, and
     $L_X \propto T_X^{4.8}$ for $T_X < 0.7$ keV.

   - $T_X \propto \sigma^{1.75}$ when $\gtrsim 10$ galaxies used to estimate σ, and
     $T_X \propto \sigma^{\approx 1}$ when 3-5 galaxies are used for the smallest groups.

   The relations with various assumptions about metallicity, surface brightness thresholds, and velocity dispersion estimates are summarized in Table 1.

11. While the amplitude of our $L_X - \sigma$ relation amplitude is in good agreement with observations, the amplitudes of our $T_X - \sigma$ and $L_X - T_X$ relations show significant discrepancies, and our median value of $\beta_{\mathrm{spec}} = 0.47$ is lower than observational estimates. We conclude that the luminosity-weighted temperatures of our simulated groups are too high by a factor of $1.5 - 2$. This discrepancy appears to originate in the central regions, with $r < 0.2R_{\mathrm{vir}}$, where observed group temperature profiles drop towards the center while our simulated profiles are flat or rising. An *ad hoc* introduction of a cool central region brings the amplitudes of both the $T_X - \sigma$ and $L_X - T_X$ relations into reasonable agreement with observations. We suspect that the ultimate origin of these discrepancies is missing physics in our simulation, such as AGN heating of the intracluster gas, but we cannot rule out numerical effects.

These results can be taken on several levels. At their most basic and most robust level, they indicate that groups cannot be treated as self-similarly scaled-down versions of clusters, since radiative cooling plays an increasingly important role in smaller systems. Although the cooling time in the outskirts of groups and clusters is longer than the Hubble time today, cooling times were shorter in the subsystems that merged to make up the final group, and even today cooling can be significant out to a non-trivial fraction of the Virial radius. Thus, the conventional approach of modeling X-ray properties with purely adiabatic physics must be applied with caution, especially as one moves from the mass regime of rich clusters to that of poor clusters and groups. Since cooling is a process that is known to occur, more

exotic processes like pre-heating or entropy injection should be examined in the context of models that already incorporate cooling. Unfortunately, this requirement increases the complexity and the uncertainty of the calculations, whether they are analytic or numerical.

At a second level, our results show that this simulation with cooling *qualitatively* reproduces the trends seen in observed scaling relations, namely a reduced luminosity of lower mass systems (relative to self-similar predictions), and a break below which the luminosity relations steepen further. While we have used numerical methods to obtain this result, it may be explained by a simple physical picture based on hierarchical growth of structure. At any epoch, the progenitor of a group will have a lower Virial temperature than the progenitor of a cluster. Hence, integrated over the formation history of these objects, a larger fraction of baryons will cool in the group environment than in the cluster environment. This results in the trends seen in the simulations and in the observations. Put another way, it is well known that in clusters most baryons are hot, while in galaxies most baryons are cold; our results simply suggest that the transition between these regimes occurs in galaxy groups around 1 keV.

At a third, more uncertain level, our results may be taken as evidence that a ΛCDM cosmological model with standard gas dynamics and radiative cooling can *quantitatively* explain observed group scaling relations, without strong pre-heating or substantial entropy injection. The uncertainty arises because our simulation does not reproduce the observations in their entirety: the forms of the predicted scalings are about right, but the mass scale of the breaks is somewhat too low, the cold gas fractions are somewhat resolution-dependent, and at a given σ the luminosity-weighted temperatures are too high. Presently, we do not know the extent to which these discrepancies reflect numerical inaccuracies, missing astrophysical processes, incorrect cosmological parameters, or errors in the observational inferences themselves. We therefore do not know whether solving these problems will reduce the role of cooling to the point that it no longer explains the observed form of the scaling relations. Definitive measurements of resolved surface brightness and gas density profiles would be a powerful diagnostic for the relative importance

of radiative cooling and non-gravitational heating in accounting for observed scaling relations.

Our simulation demonstrates that cooling can reproduce many of the qualitative features in scaling relations that are often quoted as evidence for pre-heating. Our conclusion on this point agrees with those drawn by Bryan (2000) and Voit & Bryan (2001) on the basis of analytic models and by Muanwong et al. (2001) on the basis of numerical simulations. New in this paper are the use of relatively high-resolution simulations well suited to the group mass regime and a more detailed consideration of observational issues than these earlier studies. In agreement with Bower et al. (2001), we find that cooling seems to "kick in" at a mass scale slightly smaller than required by observations. This discrepancy of mass scales may indicate that some non-gravitational heating is still required. Certainly high-redshift galaxies are observed to produce strong winds (Pettini et al. 2001), and AGN activity is sometimes seen in the centers of groups, so potential sources of non-gravitational heating do exist. Some recent models of cluster "cooling flows" incorporate an additional heat source that serves to maintain the inner gas at an intermediate temperature, suppressing the spectral signatures of ~ 1 keV gas that would otherwise be expected (David et al. 2001; Fabian et al. 2001). Hence, it is plausible that baryons in groups have experienced some non-gravitational heating, but the amount needed to reconcile models with observations may be much less than previously proposed, thus alleviating the "ICM energy crisis."

Fortunately, this field appears poised for breakthroughs on both observational and theoretical fronts. *XMM* and *Chandra* will allow studies of groups with greater sensitivity, spatial resolution, and spectral resolution than previously possible. Constraints on optical properties of groups continue to improve with deeper surveys. On the modeling side, much effort has gone into exploring solutions for the "decoupling problem" in two-phase regimes, with new algorithms being proposed that may alleviate the problem in a self-consistent fashion (e.g. Thacker et al. 2000; Springel & Hernquist 2001). Furthermore, Moore's Law improvement in computing technology continues unabated, enabling ever larger and higher resolution simulations. Advances on both

fronts will soon enable reliable side-by-side comparisons of simulations and observations, where the simulations are analyzed using exactly the same techniques as the data. This approach promises to yield an in-depth understanding of the physical processes governing the formation of galaxies in their most ubiquitous environment, groups.

REFERENCES

Allen, S. W. & Fabian, A. C. 1998, MNRAS, 297, L57

Allen, S. W., Schmidt, R. W., & Fabian, A. C. 2001, MNRAS, 328, L37

Babul, A., Balogh, M. L., Lewis, G. F., & Poole, G. B. 2002, MNRAS, 330, 329

Balogh, M. L., Pearce, F. R., Bower, R. G., & Kay, S. T. 2001, MNRAS, 326, 1228

Bernstein, R. A., Freedman, W., & Madore, B. F. 2001, ApJ, in press, astro-ph/0112193

Bialek, J. J., Evrard, A. E., & Mohr, J. J. 2001, ApJ, 555, 597

Blanton, M. R., Cen, R., Ostriker, J. P., Strauss, M. A., & Tegmark, M. 2000, ApJ, 531, 1

Blanton, M. R., et al. 2001, AJ, submitted, astro-ph/0012085

Boehringer, H., et al. A&A, 365, L181

Boehringer, H., Matsushita, K., Ikebe, Y., & Churazov, E. 2001, to appear in proc. Sesto 2001, "Tracing Cosmic Evolution with Galaxy Clusters", ed. R. Valdarnini, astro-ph/0111113

Borgani, S., Governato, F., Wadsley, J., Menci, N., Tozzi, P., Lake, G., Quinn, T., & Stadel, J. 2001, ApJ, 559, L71

Bower, R. G. 1997, MNRAS, 288, 355

Bower, R. G., Benson, A. J., Lacey, C. G., Baugh, C. M., Cole, S., & Frenk, C. S. 2001, MNRAS, 325, 497

Bryan, G. L. 2000, ApJ, 544, L1

Bryan, G. L. & Machacek, M. E. 2000, ApJ, 534, 57

Buote, D. A. 2000, MNRAS, 311, 176

Cirimele, G., Nesci, R., & Trevese, D. 1997, ApJ, 475, 11

Cole, S., et al. 2001, MNRAS, 326, 255

Croft, R. A. C., Di Matteo, T., Davé, R., Hernquist, L., Katz, N., Fardal, M. A., & Weinberg, D. H. 2001, ApJ, 557, 61

Davé, R., Dubinski, J., & Hernquist, L. 1997, NewAst, 2, 277

Davé, R. & Tripp, T. M. 2001, ApJ, 553, 528

Davé, R. et al. 2001, ApJ, 552, 473

David, L. P., Nulsen, P. E. J., McNamara, B. R., Forman, W.,

Davis, D. S., Mulchaey, J. S., & Mushotzky, R. F. 1999, ApJ, 511, 34

De Grandi, S. & Molendi, S. 2002, ApJ, 567, 163

Evrard, A. E., Metzler, C. A., & Navarro, J. F. 1996, ApJ, 469, 494

Fabian, A. C. 1994, ARA&A, 32, 277

Fabian, A. C., Mushotzky, R. F., Nulsen, P. E. J., & Peterson, J. R. 2001, MNRAS, 321, L20

Gardner, J. P. 2001, ApJ, 557, 616

Governato, F., Ghigna, S., Moore, B., Quinn, T., Stadel, J., & Lake, G. 2001, ApJ, 547, 555

Helsdon, S. F. & Ponman, T. J. 2000, MNRAS, 315, 356

Hwang, U., Mushotzky, R. F., Burns, J. O., Fukazawa, Y., & White, R. A. 1999, ApJ, 516, 604

Katz, N., Weinberg D.H., & Hernquist, L. 1996, ApJS, 105, 19

Kay, S. T., Pearce, F. R., Jenkins, A., Frenk, C. S., White, S. D. M., Thomas, P. A., and Couchman, H. M. P. 2000, MNRAS, 316, 374

Kravtsov, A. V. & Yepes, G. 2000, MNRAS, 318, 227

Lewis, G. F., Babul, A., Katz, N., Quinn, T., Hernquist, L., & Weinberg, D. H. 2000, ApJ, 536, 623

Lloyd-Davies, E. J., Ponman, T. J., & Cannon, D. B. 2000, MNRAS, 315, 689

Mahdavi, A. & Geller, M. J. 2001, ApJ, 554, L129

Mohr, J. J., Mathiesen, B., & Evrard, A. E. 1999, ApJ, 517, 627

Muanwong, O., Thomas, P. A., Kay, S. T., Pearce, F. R., & Couchman, H. M. P. 2001, ApJ, 552, L27

Mulchaey, J. S., Davis, D. S., Mushotzky, R. F., & Burstein, D. 1996, ApJ, 456, 80

Mulchaey, J. S. & Zabludoff, A. I. 1998, ApJ, 496, 73

Mulchaey, J. S. 2000, ARA&A, 38, 289

Murali, C., Katz, N., Hernquist, L., Weinberg, D. H., & Davé, R. 2002, ApJ, in press, astro-ph/0106282

Narayan, R. & Medvedev, M. V. 2001, ApJ, 562, L129

Navarro, J. F., Frenk, C. S., & White, S. D. M. 1995, MNRAS, 275, 720

Nulsen, P. E. J., David, L. P., McNamara, B. R., Jones, C., Forman, W. R., Wise, M. 2002, ApJ, 568, 163

Owen, J. M., Weinberg, D. H., Evrard, A. E., Hernquist, L., & Katz, N. 1998, ApJ, 503, 160

Pearce, F. R., Thomas, P. A., Couchman, H. M. P., & Edge, A. C. 2000, MNRAS, 317, 1029

Pearce, F. R., Jenkins, A., Frenk, C. S., White, S. D. M., Thomas, P. A., Couchman, H. M. P., Peacock, J. A., & Efstathiou, G. 2001, MNRAS, 326, 649

Pettini, M., Shapley, A. E., Steidel, C. C., Cuby, J.-G., Dickinson, M., Moorwood, Alan F. M., Adelberger, K. L., Giavalisco, M. 2001, ApJ, 554, 981

Pen, U.-L. 1999, ApJ, 510, L1

Peterson, J. R. et al. 2001, A&A, 365, L104

Phillips, L. A., Ostriker, J. P., & Cen, R. 2001, ApJ, 554, L9

Pipino, A., Matteucci, F., Borgani, S., & Biviano, A. 2002, NewAst, in press, astro-ph/0204161

Ponman, T. J., Cannon, D. B., & Navarro, J. F. 1999, Nature, 397, 135

Raymond, J. C. & Smith, B. W. 1977, ApJS, 35, 419

Ricotti, M., Gnedin, N. Y., & Shull, J. M. 2000, ApJ, 534, 41

Schaye, J., Theuns, T., Leonard, A., & Efstathiou, G. 1999, MNRAS, 310, 57

Springel, V. & Hernquist, L. 2001, ApJ, submitted, astro-ph/0111016

Thacker, R. J., Tittley, E., R., Pearce, F. R., Couchman, H. M. P., & Thomas, P. A. 2000, MNRAS, 319, 619

Thomas, P. A., Muanwong, O., Kay, S. T., & Liddle, A. R. 2002, MNRAS, 330, L48

Tovmassian, H. M., Yam, O., & Tiersch, H. 2002, ApJ, 567, L33

Tozzi, P. & Norman, C. 2001, ApJ, 546, 63

Tozzi, P. 2001, to appear in proc. Sesto 2001, "Tracing Cosmic Evolution with Galaxy Clusters", ed. R. Valdarnini, astro-ph/0109072

Valageas, P. & Silk, J. 1999, A&A, 350, 725

Voit, G. M. & Bryan, G. L. 2001, Nature, 414, 425

Voit, G. M., Bryan, G. L., Balogh, M. L., & Bower, R. G. 2002, ApJ, submitted

White, D. A., Jones, C., & Forman, W. 1997, MN-RAS, 292, 419

Wu, K. K. S., Fabian, A. C., & Nulsen, P. E. J. 2000, MNRAS, 318, 889

Wu, K. K. S., Fabian, A. C., & Nulsen, P. E. J. 2001, MNRAS, 324, 95

Xu, H., Jin, G., & Wu, X.-P. 2001, ApJ, 553, 78

Xue, Y.-J. & Wu, X.-P. 2000, ApJ, 538, 65

Zabludoff, A. I. & Mulchaey, J. S. 1998, ApJ, 496, 87

Zimer, M., Mulchaey, J. S., & Zabludoff, A. I. 2001, to appear in proc Sesto 2001, "Tracing Cosmic Evolution with Galaxy Clusters", ed. R. Valdarnini, astro-ph/0110046